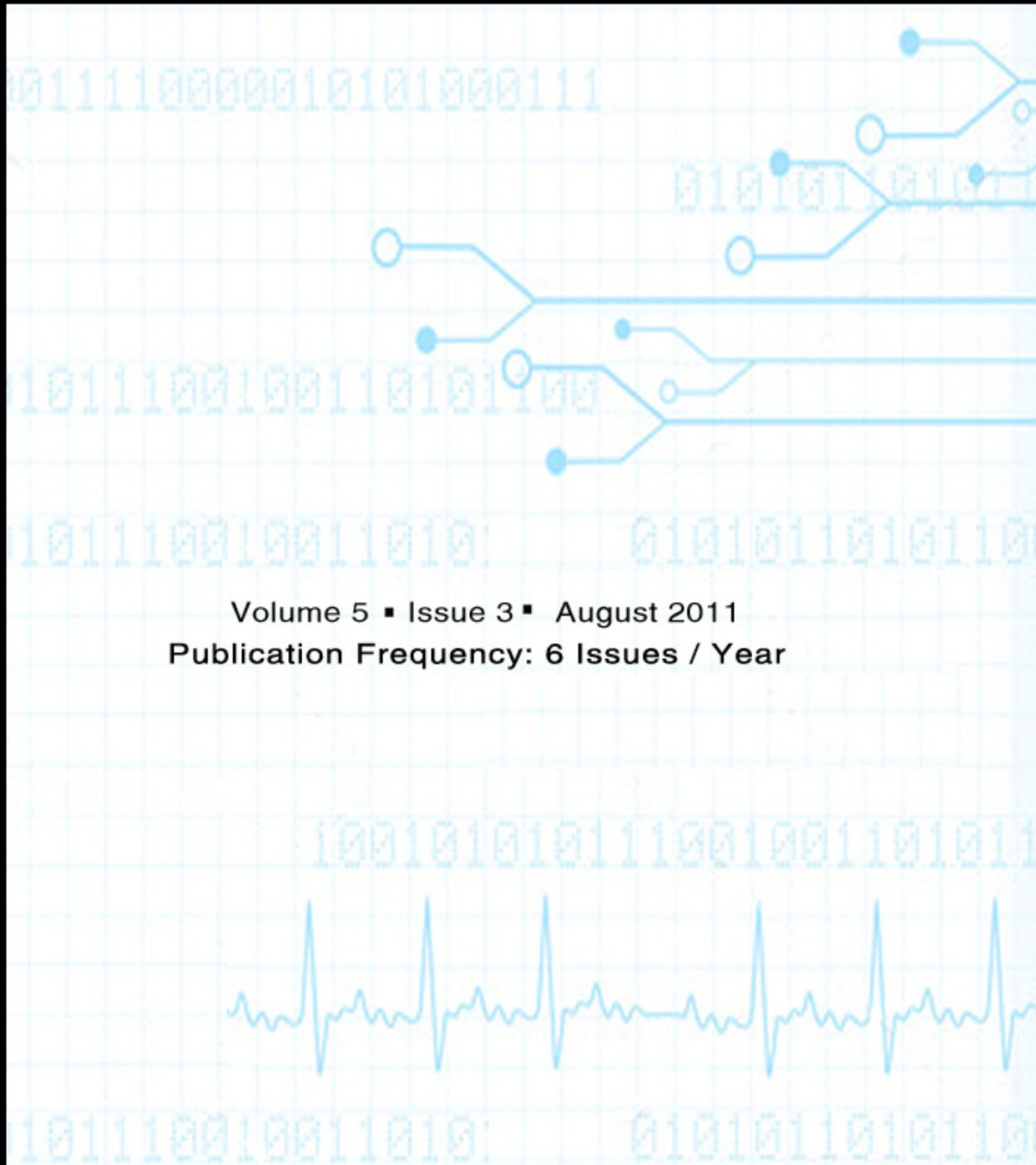


Editor-in-Chief
Dr Saif alZahir

SIGNAL PROCESSING (SPIJ)

AN INTERNATIONAL JOURNAL

ISSN : 1985-2339



Volume 5 ■ Issue 3 ■ August 2011
Publication Frequency: 6 Issues / Year

Copyrights © 2011 Computer Science Journals. All rights reserved.

CSC PUBLISHERS
<http://www.cscjournals.org>

SIGNAL PROCESSING: AN INTERNATIONAL JOURNAL (SPIJ)

VOLUME 5, ISSUE 3, 2011

**EDITED BY
DR. NABEEL TAHIR**

ISSN (Online): 1985-2339

International Journal of Computer Science and Security is published both in traditional paper form and in Internet. This journal is published at the website <http://www.cscjournals.org>, maintained by Computer Science Journals (CSC Journals), Malaysia.

SPIJ Journal is a part of CSC Publishers

Computer Science Journals

<http://www.cscjournals.org>

SIGNAL PROCESSING: AN INTERNATIONAL JOURNAL (SPIJ)

Book: Volume 5, Issue 3, August 2011

Publishing Date: 31-08-2011

ISSN (Online): 1985-2339

This work is subjected to copyright. All rights are reserved whether the whole or part of the material is concerned, specifically the rights of translation, reprinting, re-use of illustrations, recitation, broadcasting, reproduction on microfilms or in any other way, and storage in data banks. Duplication of this publication or parts thereof is permitted only under the provision of the copyright law 1965, in its current version, and permission of use must always be obtained from CSC Publishers.

SPIJ Journal is a part of CSC Publishers

<http://www.cscjournals.org>

© SPIJ Journal

Published in Malaysia

Typesetting: Camera-ready by author, data conversion by CSC Publishing Services – CSC Journals, Malaysia

CSC Publishers, 2011

EDITORIAL PREFACE

This is third issue of volume five of the Signal Processing: An International Journal (SPIJ). SPIJ is an International refereed journal for publication of current research in signal processing technologies. SPIJ publishes research papers dealing primarily with the technological aspects of signal processing (analogue and digital) in new and emerging technologies. Publications of SPIJ are beneficial for researchers, academics, scholars, advanced students, practitioners, and those seeking an update on current experience, state of the art research theories and future prospects in relation to computer science in general but specific to computer security studies. Some important topics covers by SPIJ are Signal Filtering, Signal Processing Systems, Signal Processing Technology and Signal Theory etc.

The initial efforts helped to shape the editorial policy and to sharpen the focus of the journal. Starting with volume 5, 2011, SPIJ appears in more focused issues. Besides normal publications, SPIJ intend to organized special issues on more focused topics. Each special issue will have a designated editor (editors) – either member of the editorial board or another recognized specialist in the respective field.

This journal publishes new dissertations and state of the art research to target its readership that not only includes researchers, industrialists and scientist but also advanced students and practitioners. The aim of SPIJ is to publish research which is not only technically proficient, but contains innovation or information for our international readers. In order to position SPIJ as one of the top International journal in signal processing, a group of highly valuable and senior International scholars are serving its Editorial Board who ensures that each issue must publish qualitative research articles from International research communities relevant to signal processing fields.

SPIJ editors understand that how much it is important for authors and researchers to have their work published with a minimum delay after submission of their papers. They also strongly believe that the direct communication between the editors and authors are important for the welfare, quality and wellbeing of the Journal and its readers. Therefore, all activities from paper submission to paper publication are controlled through electronic systems that include electronic submission, editorial panel and review system that ensures rapid decision with least delays in the publication processes.

To build its international reputation, we are disseminating the publication information through Google Books, Google Scholar, Directory of Open Access Journals (DOAJ), Open J Gate, ScientificCommons, Docstoc and many more. Our International Editors are working on establishing ISI listing and a good impact factor for SPIJ. We would like to remind you that the success of our journal depends directly on the number of quality articles submitted for review. Accordingly, we would like to request your participation by submitting quality manuscripts for review and encouraging your colleagues to submit quality manuscripts for review. One of the great benefits we can provide to our prospective authors is the mentoring nature of our review process. SPIJ provides authors with high quality, helpful reviews that are shaped to assist authors in improving their manuscripts.

Editorial Board Members

Signal Processing: An International Journal (SPIJ)

EDITORIAL BOARD

EDITOR-in-CHIEF (EiC)

Dr Saif alZahir

University of N. British Columbia (Canada)

ASSOCIATE EDITORS (AEiCs)

Professor. Wilmar Hernandez

Universidad Politecnica de Madrid
Spain

Dr. Tao WANG

Universite Catholique de Louvain
Belgium

Dr. Francis F. Li

The University of Salford
United Kingdom

EDITORIAL BOARD MEMBERS (EBMs)

Dr. Thomas Yang

Embry-Riddle Aeronautical University
United States of America

Dr. Jan Jurjens

University Dortmund
Germany

Dr. Jyoti Singhai

Maulana Azad National institute of Technology
India

TABLE OF CONTENTS

Volume 5, Issue 3, August 2011

Pages

- 80 - 92 Performance Comparison of Known ICA Algorithms to A Wave-let ICA Merger
Janett Walter-Williams, Yan Li
- 93 – 100 Noisy Speech Enhancement Using Soft Thresholding On Selected Intrinsic Mode Functions
Hadhami Issaoui, Aicha Bouzid, Nouredine Ellouze
- 101 - 109 Classification of Cardiac Arrhythmia Using WT, HRV and Fuzzy C-Means Clustering
A. Dallali, A.Kachouri, M. Samet
- 110 - 119 Power Efficiency Improvement in CE-OFDM System with 0 db IBO For Transmission over PLC Network
El Ghzaoui, Belkaid Jamil, Benbassoui Ali, EL Bekkali Molhim
- 120 - 129 An Approach To reduce Noise in Speech Signals Using An Intelligent System: BELBIC
Edet Bijoy K, Musfir Mohammad

Performance Comparison of Known ICA Algorithms to a Wavelet-ICA Merger

Janett Walters-Williams

*School of Computing & Information Technology
Faculty of Engineering & Computing
University of Technology, Jamaica
237 Old Hope Road, Kingston 6, Jamaica W.I.*

jwalters@utech.edu.jm

Yan Li

*Department of Mathematics & Computing
Faculty of Sciences
University of Southern Queensland
Toowoomba, Australia*

liyan@usq.edu.au

Abstract

These signals are however contaminated with artifacts which must be removed to have pure EEG signals. These artifacts can be removed by Independent Component Analysis (ICA). In this paper we studied the performance of three ICA algorithms (FastICA, JADE, and Radical) as well as our newly developed ICA technique. Comparing these ICA algorithms, it is observed that our new techniques perform as well as these algorithms at denoising EEG signals.

Keywords: Independent Component Analysis, Wavelet Transform, Unscented Kalman Filter, Electroencephalogram

1. INTRODUCTION

The use of Electroencephalogram in the field of Medicine has had a great impact on the study of the human brain. The signals received have several origins however that lead to the complexity of their identification. This complexity is made of both the pure EEG signal and other non-cerebral signals called artifacts or noise. The artifacts have resulted in the contamination of the EEG signals, hence the removal of these artifacts has generated a large number of denoising techniques.

One method has been Independent Component Analysis (ICA) originating from the field of Blind Source Separation [5]. This technique calls for the separation of the EEG into its constituent independent components (ICs) and then eliminating the ICs that are believed to contribute to the artifact sources. It is subjective, inconvenient and a time consuming process when dealing with large amount of EEG data. Another method employed is wavelet transformation. This technique calls for the decomposition of the EEG signals into wavelets and artifacts removal done using thresholding and shrinkage.

Each of the above techniques presents their own limitations. In our opinion a combination of the two should produce a more effective technique. This is possible as each technique is used to overcome the limitation of the other. We present in this paper therefore a new method of extracting artifacts from EEG signals – Cycle Spinning Wavelet Transform ICA (CTICA). CTICA is compared to other known ICA algorithms, and saving useful EEG data.

2. SUPPORTING LITERATURE

2.1 EEG Signals

The language of communication with the nervous system is electric so when the neurons of the human brain process information, they do so by changing the flow of electrical currents across their membranes. These changing currents generate electric and magnetic fields that can be recorded from the surface of the scalp. The electric fields are measured by attaching small electrodes to the scalp. The potentials between different electrodes are then amplified and recorded as the electroencephalogram; (EEG), which means the writing out of the electrical activity of the brain (that which is inside the head). EEG recordings therefore, show the overall activity of the millions of neurons in the brain.

There are five basic wave types, measured in Hertz (HZ), found in EEG signals (Tab. 1). The most prominent type is the alpha rhythm recorded mainly over the posterior regions of the scalp close to the places in the brain that process visual information. When the eyes are open the alpha rhythm is very small and when the eyes are closed it becomes large.

Type	Frequency(Hz)	Normally
Delta (δ)	0.5-4 Hz	Deep, dreamless sleep, non-REM sleep, unconscious
Theta (θ)	4 – 8 Hz	Intuitive, creative, recall, fantasy, imaginary, dream
Alpha (α)	8 – 13 Hz	Relaxed, but not drowsy, tranquil, conscious
Beta (β)	13 – 30 Hz	Formerly SMR, relaxed yet focused, integrated, Thinking, aware of self & surroundings, Alertness, agitation
Gamma (γ)	30 – 100+ Hz	Motor Functions, higher mental activity

TABLE 1: Wave Types Found in EEG Signals (*adapted from Neurosky Inc. 2009 Brain Wave Signal (EEG) of NeuroSky, Inc.*)

Since an EEG is used to analyzed brain function it is used in clinical practice to:

- (i) Diagnose epilepsy and see what type of seizures is occurring. EEG is the most useful and important test in confirming a diagnosis of epilepsy.
- (ii) Check for problems with loss of consciousness or dementia.
- (iii) Help find out a person's chance of recovery after a change in consciousness.
- (iv) Find out if a person who is in a coma is brain-dead.
- (v) Study sleep disorders, such as narcolepsy.
- (vi) Watch brain activity while a person is receiving general anesthesia during brain surgery.
- (vii) Help find out if a person has a physical problem (problems in the brain, spinal cord, or nervous system) or a mental health problem.

Being a physical system however, EEG is subjected to random disturbance. The measurements or observations are generally contaminated with other non-cerebral signals called artifacts or noise caused by the electronic and mechanical components of the measuring devices. These may include EOG (Eye-induced) artifacts (includes eye blinks and eye movements); EKG (Fig 1) (cardiac) artifacts; EMG (muscle activation)-induced artifacts; and Glossokinetic (chewing & sucking movement) artifacts. Artifacts sometimes mimic EEG signals and overlay these signals resulting in distortion making analysis impossible. In clinical practice areas in the reading with artifacts are cancelled resulting in considerable information loss, thus sometimes resulting in misdiagnosis.

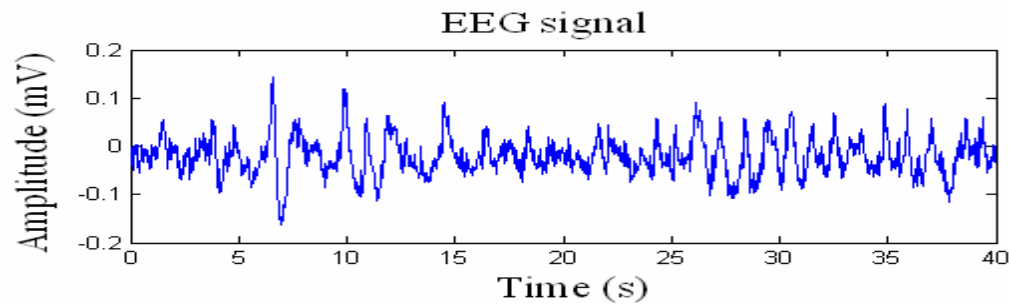


FIGURE 1: EEG Signal corrupted with ECG/EKG and line signals (*adapted from Artifact Removal from EEG Signals using Adaptive Filters In Cascade, A Garcés Correa et al, Journal of Physics: Conference Series 90, 2007*)

Artifacts must be eliminated or attenuated to ensure correct analysis and diagnosis. Through the years there have been different methods of denoising such as artifacts rejection, regression and Principal Components Analysis (PCA). More recently two other methods have been discussed – Independent Component Analysis (ICA) and Wavelet Transform (WT).

2.2 Independent Component Analysis

When a signal is contaminated it is a combination of the true signal $S(t)$ and the artifacts $\varepsilon(t)$ producing equation (1) where $c(t)$ is the contaminated signal.

$$c(t) = S(t) + \varepsilon(t) \quad (1)$$

Researchers have been utilizing ICA to remove $\varepsilon(t)$.

ICA is an extension of PCA which originated from the field of Blind Source Separation. It is suitable for performing source separation where

- (i) sources are independent
- (ii) propagation delays of mixing medium are negligible
- (iii) source are analog with pdfs not too unlike the gradient of a logistic sigmoid
- (iv) the number of independent signals sources is the same as the number of sensors.

Investigations show that EEG satisfies (i) since there are statistically independent brain processes, (ii) since the volume conduction in the brain tissue is efficiently instantaneous. The assumption of (iii) is plausible but the assumption that EEG signals are a linear mixture of exactly N sources is questionable since we do not know the effective number of statistically independent brain signals contributing to the EEG recorded from the scalp [19]. ICA can therefore be used to performance separations on these signals. There are problems with using ICA however

- (i) Its performance depends however on the length of the dataset, because the larger the set the more likely person will have to deal with an over complete ICA which cannot separate artifacts from the signals.
- (ii) When ICA performs separations sometimes some useful signals maybe removed as a part of the artifacts resulting in information loss [11].

2.3 Wavelet Transform

Wavelet analysis, a sub brand of applied mathematics has been used to decompose signals in the time frequency scale plane (fig 2). It has been found to be an efficient technique for non-stationary signal processing of which EEG falls. [1] [22]. Its capability to transform the EEG time domain signal into time and frequency localization helps researchers understand more the behaviour of the signals.

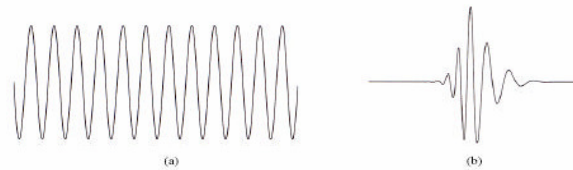


FIGURE 2: Demonstration of (a) a wave and (b) a wavelet. Notice that the wave has an easily discernible frequency while the wavelet has a *pseudo frequency* in that the frequency varies slightly over the length of the wavelet. (adapted from D.L. Fugal. 2009. *Conceptual Wavelets in Digital Signal Processing: An in depth Practical Approach for the Non-Mathematician*, Space & Signals Technologies LLC)

There are two basic types of wavelet transform. One type of wavelet transform is designed to be easily reversible (invertible); that means the original signal can be easily recovered after it has been transformed. This kind of wavelet transform is used for image compression and cleaning (noise and blur reduction). Typically, the wavelet transform of the image is first computed, the wavelet representation is then modified appropriately, and then the wavelet transform is reversed (inverted) to obtain a new image.

The second type of wavelet transform is designed for signal analysis for study of EEG or other biomedical signals. In these cases, a modified form of the original signal is not needed and the wavelet transform need not be inverted (it can be done in principle, but requires a lot of computation time in comparison with the first type of wavelet transform). Decomposition- into wavelets is done by a “mother and “father” wavelet function. These “mother” functions include Haar, Daubechies and Mexican Hat. Equation (2) shows that it is possible to build a wavelet for any function by dilating the mother wavelet function $\psi(t)$ with a coefficient 2^j , and translating the resulting function on a grid whose interval is proportional to 2^{-j} .

$$\Psi_{(a,b)}(t) = 2^{\frac{a}{2}} \psi(2^a t - b) \quad (2)$$

Compressed versions of the wavelet function match the high-frequency components, while stretched versions match the low-frequency components. By correlating the original signal with wavelet functions of different sizes, the details of the signal can be obtained at several scales or moments. These correlations with the different wavelet functions can be arranged in a hierarchical scheme called multi-resolution decomposition. The multi-resolution decomposition algorithm separates the signal into “details” at different moments and wavelet coefficients [22] [23]. These coefficients are called the Discrete Wavelet Transform (DWT) of the signal. As the moments increase the amplitude of the discrete details become smaller however the coefficients of the useful signals increase [27] [28].

If the details are small enough they might be omitted without substantially affecting the main signals. This omission is done through Thresholding. There are two main ways to denoise a signal in WT – soft and hard thresholding. Research as shown that soft-thresholding has better mathematical characteristics [27] [28] and provides smoother results [9]

2.4 Unscented Kalman Filter

Unscented Kalman Filter (UKF) is a Bayesian filter which uses minimum mean-squared error (MMSE) as the criterion to measure optimality [4][34]. For highly nonlinear systems, the linear estimate of the nonlinear model does not provide a good approximation of the model, and the Extended Kalman Filter (EKF) will not track signals around sharp turning points. Another problem with the EKF is that the estimated covariance matrix tends to underestimate the true covariance matrix and therefore risks becoming inconsistent in the statistical sense without the addition of "stabilising noise". UKF was found to address these flaws. It involves the Unscented Transformation (UT), a method used to calculate the first and second order statistics of the outputs of nonlinear systems with Gaussian. The nonlinear stochastic system used for the algorithm is:

$$\begin{aligned}x_{k+1} &= A x_k + B u_k + v_k \\y_k &= H x_k + w_k\end{aligned}\quad (3)$$

where A and H are the known and constant matrices respectively, x_k is the unobserved state of the system, u_k is a known exogenous input, y_k is the observed measurement signal, v_k is the process noise and w_k is the measurement noise.

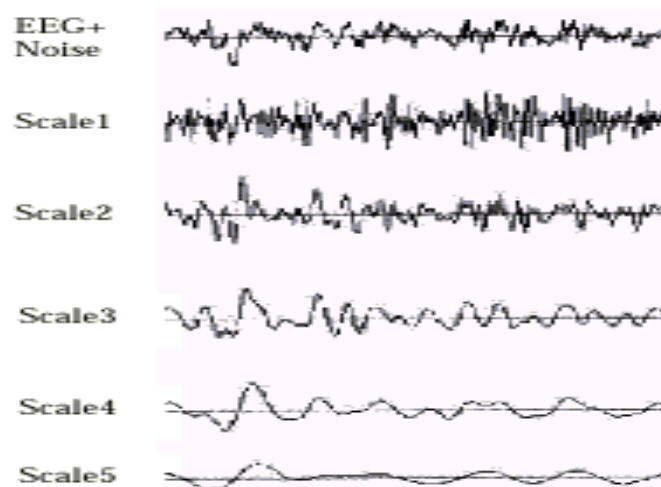


FIGURE 3: Noisy EEG and its Wavelet Transform at different scales (*adapted from Weidong Z., Yingyuan, L. 2001. EEG Multi-resolution Analysis using Wavelet Transform, 23rd Annual International Conference of the IEEE Engineering in Medicine and Biology Society (IEEE/EMBS) 2001*)

UKF uses the intuition that it is easier to approximate a probability distribution function rather than to approximate an arbitrary nonlinear function or transformation. Following this intuition, a set of sample points, called sigma points, are generated around the mean, which are then propagated through the nonlinear map to get a more accurate estimation of the mean and covariance of the mapping results. In this way, it avoids the need to calculate the Jacobian, which for complex functions can be a difficult task in itself (i.e., requiring complicated derivatives if done analytically or being computationally costly if done numerically).

3. PREVIOUS RESEARCH

WT and ICA in recent years have often been used in Signal Processing. [22] [27]. Although ICA is popular and for the most part does not result in much data loss; its performance depends on the size of the data set i.e. the number of signals. The larger the set, the higher the probability that

the effective number of sources will overcome the number of channels (fixed over time), resulting in an over complete ICA. This algorithm might not be able to separate noise from the signals. Another problem with ICA algorithms has to do with the signals in frequency domain. Although noise has different distinguishing features, once they overlap the EEG signals ICA cannot filter them without discarding the true signals as well. This results in data loss.

WT utilizes the distinguishing features of the noise however. Once wavelet coefficients are created, noise can be identified. Decomposition is done at different levels (L); DWT produces different scale effects (Fig 3). Weidong et al. [25] proved that as scales increase the WT of EEG and noise present different inclination. Noise concentrates on scale 21, decreasing significantly when the scale increases, while EEG concentrates on the 22-25 scales. Elimination of the smaller scales denoise the EEG signals. WT therefore removes any overlapping of noise and EEG signals that ICA cannot filter out.

More recently there has been research comparing the denoising techniques of both. It was found

- (i) If artifacts and signals are nearly the same or higher amplitude, wavelets had difficulty distinguishing them. ICA on the other hand looks at the underlying distributions thus distinguishing each [29].
- (ii) ICA gives high performance when datasets are large. It suffers from the trade off between a small data set and high performance [11].

Research therefore shows that ICA and wavelets complement each other, removing the limitations of each [29]. Since then research as been done applying a combination of both with ICA as a per- or post- denoising tool. Inuso *et al.* [11] used them where ICA and wavelets are joint. They found that their method outperformed the pre- and post- ICA models.

4. RESEARCH DATASETS

EEG data was taken from two sites

- (i) http://sccn.ucsd.edu/~arno/fam2data/publicly_available_EEG_data.html. The signals from here are contaminated with EOG. Data is sampled at a rate of 128 samples per second recorded from 32 electrodes at 1000Hz
- (ii) <http://www.filewatcher.com/b/ftp/ftp.ieee.org/uploads/press/rangayyan.0.0.html>. Data was collected at a sampling rate of 1000Hz but noise free. These signals had to artificially contaminated

These two sites produce signals of different sizes as well as 1D and 2D signals.

5. METHODOLOGY

When a signal is decomposed it is represented as a set of wavelet coefficients that correlates to high frequency sub-bands. Artifacts are usually of low frequency and can be removed by shrinkage or thresholding. Research has shown however that thresholding has a slow response [22] [23]. In this paper we are presently another method to denoising using WT and ICA. Some of the ideas appear in earlier algorithms however the main difference of CTICA is the use of cycle spinning; the merger of Wavelet Transform and ICA into one and the improvement of denoising.

The presented method is based on decomposition by using Symmlets which is a near symmetric extension of Daubechies. Symlets are orthogonal and its regularity increases with the increase in the number of moments [6]. After experiments the number of vanishing moments chosen is 8 (Sym8).

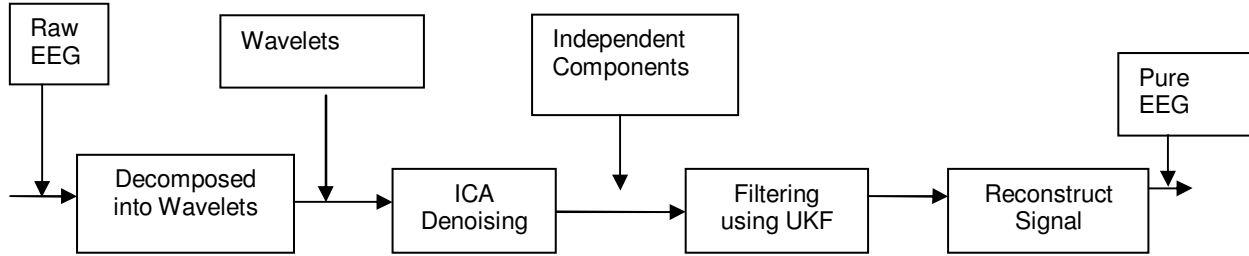


FIGURE 4: Proposed Artifacts Removal System

A block diagram representation of the proposed work is shown in FIGURE 4. EEGs are acquired and Cycle Spinning applied. Cycle Spinning utilizes the periodic time invariance of the wavelet transform to separate noise from signals. The EEG signals are then decomposed by Forward DWT using the Symmlet family of wavelets. The wavelet coefficients are separated into statistically independent sources using ICA and denoising takes place. Each IC is then filtered using UKF. Finally, the sources that are identified as non-artifacts are used to reconstruct the artifact-free EEGs and Cycle Spinning applied again.

6. RESULTS & DISCUSSION

We conducted experiments, using the above mentioned signals, in Matlab 7.8.0 (R2009) on a laptop with AMD Athlon 64x2 Dual-core Processor 1.80GHz. Noisy signals were generated by adding noise to the original noise-free signals and the length of all signals, N , were truncated to lengths of power of twos i.e. 2^x .

FastICA	Jade	Radical	CT-ICA
4.1954	4.1909	4.1865	4.1912
7.1276	7.1191	7.1106	7.1192
5.1226	5.1281	5.1226	5.1278
8.0569	8.0484	8.0399	8.0487
7.8736	7.8827	7.8736	7.8815
3.5646	3.5696	3.5646	3.5703
6.0995	6.1057	6.0995	6.1042
2.733	2.7364	2.733	2.7361
0.1374	0.1373	0.1372	0.1373
8.658	8.6521	8.6462	8.6499
0.284	0.2841	0.284	0.2841
0.2234	0.2235	0.2234	0.2235
3.2436	3.2395	3.2355	3.2387

TABLE 2: MSE for 13 EEG signals (x.xe+07)

6.1 Testing Against Known ICA Algorithms

We compared the performance of our method with several state-of-the art ICA algorithms - FastICA, Radical, and Jade. All the algorithms were downloaded from the web sites of the respective authors. In the case of FastICA a symmetrical view based on the tan score function was used for comparison. To determine the quality of each signal the Mean Square Error (MSE), the Peak Signal to Noise Ratio (PSNR), the Signal to Distortion Ratio (SDR), the Signal to noise Ratio (SNR) and the Amari Performance Index were calculated.

MSE measures the average of the square of the "error" and defined as:

$$MSE = \frac{1}{MN} \sum_{y=1}^M \sum_{x=1}^N [I(x, y) - \hat{I}(x, y)]^2 \tag{4}$$

The error is the amount by which the estimator differs from the quantity to be estimated. The difference occurs because of randomness or because the estimator doesn't account for information that could produce a more accurate estimate. TABLE 2 shows the MSE for 13 signals. Observations show that there is not much difference in the MSE for each algorithm. The lower the MSE the lesser the error on the signal; it can be seen that on average our method performed better than FastICA and Jade. Radical had a lower MSE.

FastICA	Jade	Radical	CT-ICA
-18.0969	-18.0923	-18.0877	-18.0926
-20.3987	-20.3935	-20.3883	-20.3935
-18.9641	-18.9687	-18.9641	-18.9685
-20.9309	-20.9263	-20.9217	-20.9265
-20.8309	-20.836	-20.8309	-20.8353
-17.3893	-17.3954	-17.3893	-17.3962
-19.7221	-19.7266	-19.7221	-19.7255
-16.2355	-16.241	-16.2355	-16.2405
-23.2477	-23.2453	-23.243	-23.2442
-21.2434	-21.2404	-21.2375	-21.2393
-26.4025	-26.4042	-26.4025	-26.404
-25.359	-25.3609	-25.359	-25.3611
-16.9794	-16.974	-16.9686	-16.9729

TABLE 3: PSNR for 13 EEG signals

PSNR is the ratio between the maximum possible power of a signal and the power of corrupting noise that affects the fidelity of its representation. It is defined as:

$$PSNR = 10 \times \log_{10} \left(\frac{MAX^2}{MSE} \right) \tag{5}$$

Because many signals have a very wide dynamic range, PSNR is usually expressed in terms of the logarithmic decibel scale. In this research MAX takes the value of 255. Tab 3 shows the PSNR for 13 signals. If the PSNR is high then the ratio of signal to noise is higher and therefore the algorithm is considered good.

After experiments it can be seen that our algorithm has the same PSNR on average. It was also seen that it has a higher PSNR than Jade and Radical. The similar signal to noise ratio can be seen in the SNR graph in figure 5 where only Jade has a different value.

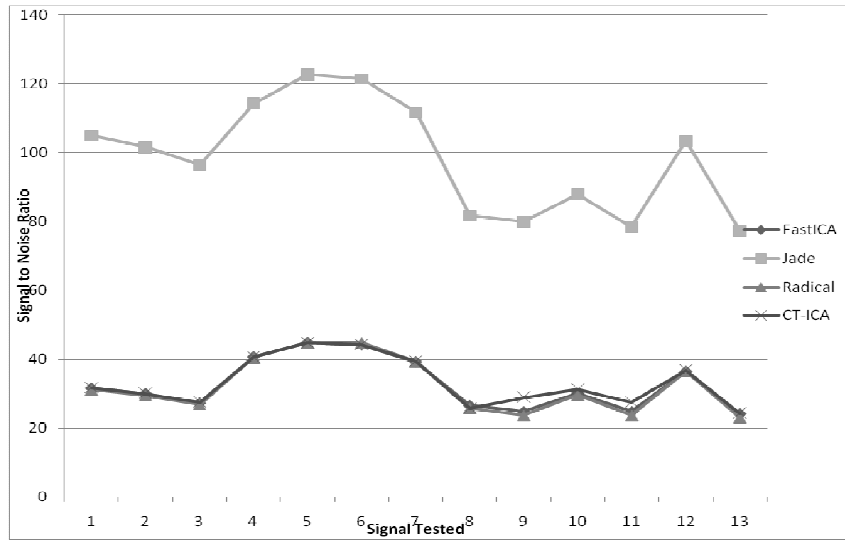


FIGURE 5: SNR results for 13 signals

The accuracy of the separation for each algorithm in terms of the signals can be calculated by the total SDR defined as:

$$SDR(x_i, y_i) = \frac{\sum_{n=1}^L x_i(n)^2}{\sum_{n=1}^L (y_i(n) - x_i(n))^2} \quad i = 1, \dots, m \quad (6)$$

where $x_i(n)$ is the original source signal and $y_i(n)$ is the reconstructed signal. When SDR are calculated any found below 8-10dB are considered to fail separation. Fig 5 shows that all four algorithms had SDR above 8dB. It also shows that CTICA had SDR very close to the other four so that there was no differentiation in the graph.

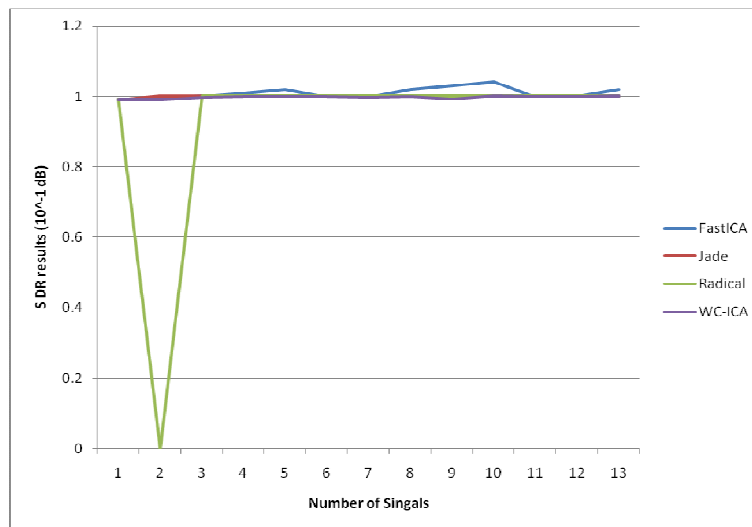


FIGURE 6: SDR results for 13 signals

The global accuracy of the separation of each algorithm was tested using the Amari performance index defined as:

$$P_{err} = \frac{1}{2m} \sum_{i,j=1}^m \left(\frac{|p_{ij}|}{\max_k |p_{ik}|} + \frac{|p_{ij}|}{\max_k |p_{kj}|} \right) - 1 \tag{7}$$

where $p_{ij} = (BA)_{ij}$. It assesses the quality of the de-mixing matrix **W** for separating observations generated by the mixing matrix **A**. The lower the Amari index, the more accurate the separation is. We have normalized all values of the Amari index to be between 0 and 1 (the max). The Amari indexes obtained for the different algorithms and for different sample sizes are presented in TABLE 4. Observations show that the Amari indexes for our method is very similar to those of Jade and FastICA. On average however it has a lower Amari than both FastICA and Jade but not Radical.

FastICA	Jade	Radical	CT-ICA
1238	1237	1236	1237
1583	1582	1581	1582
1363	1363	1363	1363
1669	1668	1667	1668
1652	1653	1652	1653
1140	1141	1140	1141
1477	1478	1477	1478
989	990	989	990
2069	2068	2068	2068
1720	1720	1719	1720
2683	2683	2683	2683
2471	2471	2471	2471
1085	1085	1084	1084

TABLE 4: Amari Test Results for 13 EEG signals (x.xe-05)

6.2 Testing against Known WT-influenced Algorithms

Zhou et al. [28] in 2004 found that a combination of wavelet threshold de-noising and ICA resulted in the removal of electromyogram (EMG) and electrocardiograph (ECG) artifacts from EEG signals. Further research in 2007 by Inuso et al. [11] resulted in the creation of a new technique for EEG artifact removal, based on the joint use of Wavelet transform and Independent Component Analysis (WICA). After comparison to pre- and post- ICA and wavelet denoising using artificial artifact-laden EEG datasets they found that this combination had the best artifact separation performance for every kind of artifact also allowing for the minimum information loss. These show that a merger of WT and ICA is more effective.

Pre-WT	Post-WT	WT-UKF	WT-ICA	CT-ICA
33.9443	1.1158e3	1.1025	1.1051	1.0947
29.0936	1.0438	1.0499	1.0379	1.0372
23.9498	1.0058	997.4019	982.4991	979.2423

TABLE 5: Sample MSE for 3 EEG signals

Sameni et al. [21] experimented with denoising using EKF on ECG data. They found that the results show that the EKF may be used as a powerful tool for the extraction of the ECG signals from noisy measurements. Jacob and Martin [12] tested a combination of WT and Weiner Filter. They concluded that this combination basic denoising using only WT

Pre-WT	Post-WT	WT-UKF	WT-ICA	CT-ICA
32.8231	17.655	17.7071	17.6966	17.7377
33.4928	17.9446	17.9192	17.9693	17.9722
34.3378	18.1058	18.1421	18.2075	18.2219

TABLE 6: Sample PSNR for 3 EEG signals

As stated before ICA and WT complement each other, removing the limitations of each [29]; researchers have shown that the combination of WT and ICA is more effective than ICA or WT alone supporting this theory. They have also shown that the performance of WT improves with the addition of Filters. In our research investigations have shown that when compared to the post- and pre- ICA models, a combination of WT with (i) ICA, or (ii) UKF we have found as seen in Tables 5 and 6 that the merger of all three outperformed all except the Pre-ICA model. This conforms to the findings of researchers.

7. CONCLUSION

In recent years researchers have used both ICA algorithms and WT to denoise EEG signals. In this paper we propose a new method – Cycle Spinning Wavelet Transform ICA (CTICA). From the experiments we can conclude the following for CTICA

- (I) It can be seen from the experiments that it can successfully separate noise from EEG signals.
- (II) It has outperformed FastICA and JADE as far as MSE was concerned,
- (III) It has outperformed JADE and Radical with PSNR.
- (IV) It has the similar in SDR and Amari index
- (V) It outperforms different WT model designs except for the Pre-ICA model.

Based on these results it can be concluded that CTICA has an overall performance which is better than all three ICA algorithms and most WT model, i.e. it is the most consistent and robust denoising method.

8. REFERENCES

- [1] M. Alfaouri and K. Daqrouq. "ECG Signal Denoising By Wavelet Transform Thresholding". American Journal of Applied Sciences 5 (3), pp. 276-281, 2008.
- [2] Z. Chen, "Bayesian Filtering: From Kalman Filters to Particle Filters, and Beyond". Adaptive Systems Lab., McMaster University., Hamilton, Ontario, Canada. Internet: http://users.isr.ist.utl.pt/~jpg/tfc0607/chen_bayesian.pdf. 2003, [Jun 20, 2009]
- [3] S. Choi, A. Cichocki, L. Zhang, and S. Amari. "Approximate Maximum Likelihood Source Separation Using the Natural Gradient". In Proc. IEEE Workshop on Signal Processing Advances in Vireless Communications, (Taoyuan, Taiwan), 2001, pp. 235-238.
- [4] R.R. Coifman, and D.L. Donoho. "Translation Invariant Denoising". Lecture Notes in Statistics: Wavelets and Statistics, pp. 125-150. 1995.
- [5] P. Comon. "Independent Component Analysis, a new concept?" Signal Processing, Elsevier, 36(3), pp. 287-314, 1994.
- [6] B. Ferguson and D. Abbott. "Denoising Techniques for Terahertz Response of Biological Samples". Microelectronics Journal 32, pp. 943-953, 1991.
- [7] N. Gadhok and W. Kinsner. "Robust ICA for Cognitive Informatics". International Journal of Cognitive Informatics and Natural Intelligence (*IJCINI*) 2(4), pp. 86-92, 2008.

- [8] Y.M. Hawwar, A.M. Reza, and R.D. Turney. "Filtering(Denoising) in the Wavelet Transform Domain". Unpublished, Department of Electrical Engineering and Computer Science, University of Wisconsin-Milwaukee, 2002.
- [9] A. Graps. "An Introduction to Wavelets". IEEE Journal of Computational Science and Engineering 2(2), pp. 1-17, 1995.
- [10] G.G. Herrero, and K. Egiazarian. "Independent Component Analysis by a Resampling Strategy". Internet: <http://www.cs.tut.fi/~gomezher/projects/bss/rica/rica.pdf>, 2005 [Sep 18, 2009]
- [11] G. Inuso, F. La Foresta, N. Mammone, and F.C. Morabito. "Wavelet-ICA methodology for efficient artifact removal from Electroencephalographic recordings". In Proc International Joint Conference on Neural Networks, 2007, pp. 1524-1529.
- [12] N. Jacob, and A. Martin. "Image Denoising in the Wavelet Domain Using Wiener Filtering". Unpublished course project, University of Wisconsin, Madison, Wisconsin, USA, 2004.
- [13] S. Julier, and J.K. Uhlmann. "Unscented Filtering and Nonlinear Estimation". In Proc IEEE 92(3), 2004, pp. 401-421.
- [14] S. Julier and J.K. Uhlmann. "A New Extension of the Kalman Filter to Nonlinear Systems". In Proceedings of AeroSense: In 11th International Symposium on Aerospace/Defense Sensing, Simulation and Controls, 1997, pp. 182-193.
- [15] A. Kallapur, S. Anavatti, and M Garratt. "Extended and Unscented Kalman Filters for Attitude Estimation of an Unmanned Aerial Vehicle". In Proc 27th IASTED International Conference on Modelling, Identification, and Control (MIC 2008), 2008.
- [16] Kaur, L., Gupta, S., & Chauhan, R.C., "Image Denoising using Wavelet Thresholding". In Proc 3rd Indian Conference on Computer Vision, Graphics & Image Processing (ICVGIP 2002), 22(14), 2002.
- [17] V. Krishnaveni, S. Jayaraman, A. Gunasekaran and K. Ramadoss. "Automatic Removal of Ocular Artifacts using JADE Algorithm and Neural Network". International Journal of Intelligent Systems and Technologies 1(4), pp. 322-333, 2006.
- [18] V. Krishnaveni, S. Jayaraman, S. Aravind, V. Hariharasudhan, and K. Ramadoss. "Automatic Identification and Removal of Ocular Artifacts from EEG using Wavelet Transform". Measurement Science Review 6(2, 4), pp. 45-57, 2006
- [19] S. Makeig, J. Anthony, A.J. Bell, T. Jung, and T.J. Sejnowski. "Independent Component Analysis of Electroencephalographic data". Advances in Neural Information Processing Systems 8, MIT Press Cambridge MA 8, pp. 145-151, 1996.
- [20] N. Nikolaev and A. Gotchev. "ECG Signal Denoising using Wavelet Domain Wiener Filtering". In Proc 10th European Signal Processing Conference (EUSIPCO 2000), 2000.
- [21] R. Sameni and M.B. Jutten. "Filtering Electrocardiogram Signals using the Extended Kalman Filter". In Proc 27th IEEE Engineering in Medicine and Biology (EMBS) Annual Conference 2005, pp. 5639-5642.
- [22] P. Senthil Kumar, R. Arumuganathan, K. Sivakumar, and C. Vimal. "A Wavelet based Statistical Method for De-noising of Ocular Artifacts in EEG Signals". International Journal of Computer Science and Network Security (IJCSNS). 8(9), pp. 87-92, 2008.

- [23] P. Senthil Kumar, R. Arumuganathan, K. Sivakumar, and C. Vimal. "Removal of Ocular Artifacts in the EEG through Wavelet Transform without using an EOG Reference Channel". *International Journal of Open Problems in Computer Science & Mathematics (IJOPCM)* 1(3), pp. 189-198, 2008.
- [24] P. Shui and Y. Zhao. "Image Denoising Algorithm using Doubling Local Wiener Filtering with Block Adaptive Windows in Wavelet Domain". *Signal Processing* 87(7), pp. 1721-1734, 2007.
- [25] Z. Weidong and L. Yingyuan.. 2001. "EEG Multi-resolution Analysis using Wavelet Transform", In Proc 23rd Annual International Conference of the IEEE Engineering in Medicine and Biology Society (IEEE/EMBS) 2001.
- [26] G. Welch and G. Bishop. "An Introduction to the Kalman Filter", Technical Report TR 95-041, University of North Carolina, Chapel Hill, North Carolina, USA. Internet: http://www.cs.unc.edu/~welch/media/pdf/kalman_intro.pdf 2006, [Aug 29, 2009]
- [27] J. Zhao, Q. Xi, X. Wang, and Y. Yang. "Image Denoising via Wavelet Domain Wiener filter based on Coorelation Model". In 16th World Conference on Nondestructive Testing (WCNDT 04), 2004.
- [28] W. Zhou and J. Gotman. "Removal of EMG and ECG Artifacts from EEG Based on Wavelet Transform and ICA". In Proc 26th Annual International Conference on the IEEE EMBS, 2004, pp. 392-395.
- [29] W. Zhou and J. Gotman. "Removing Eye-movement Artifacts from the EEG during the Intracarotid Amobarbital Procedure". *Epilepsia* 46(3), pp. 409-411, 2005.
- [30] G. Zouridakis and D. Iyer. "Comparison between ICA and Wavelet-based Denoising of single-trial evoked potentials". In Proc 26th Annual International Conference of the IEEE Engineering in Medicine and Biology Society, 2004, pp. 87-90.

Noisy Speech Enhancement Using Soft Thresholding on Selected Intrinsic Mode Functions

Hadhami Issaoui

*Electrical Engineering Department
National School of Engineers of Tunis
Le Belvédère B.P. 37, 1002 Tunis, Tunisia*

issaouihadhami@yahoo.fr

Aïcha Bouzid

*Electrical Engineering Department
National School of Engineers of Tunis
Le Belvédère B.P. 37, 1002 Tunis, Tunisia*

bouzidacha@yahoo.fr

Noureddine Ellouze

*Electrical Engineering Department
National School of Engineers of Tunis
Le Belvédère B.P. 37, 1002 Tunis, Tunisia*

N.Ellouze@enit.rnu.tn

Abstract

In this paper, a new speech enhancement method is introduced. It is essentially based on the Empirical Mode Decomposition technique (EMD) and a soft thresholding approach applied on selected modes. The proposed method is a fully data driven approach. First the noisy speech signal is decomposed adaptively into intrinsic oscillatory components called Intrinsic Mode Functions (IMFs) by using a time decomposition called sifting process. Second, selected IMFs are soft thresholded and added to the remaining IMFs with the residue to reconstitute the enhanced speech signal. The proposed approach is evaluated using speech signals from NOISEUS database corrupted with additive white Gaussian noise. Our algorithm is compared to other state of the art algorithms.

Keywords: Empirical Mode Decomposition, Speech Enhancement, Soft Thresholding, Mode-Selection.

1. INTRODUCTION

Speech enhancement is a challenging task aiming to suppress noise and to improve the perceptual quality and intelligibility of the speech signal through the noise removal. In the literature, various speech enhancement algorithms have been proposed to improve the performances of modern communications devices, particularly, in the case of additive white Gaussian noise [1, 2, 3, 4, 5].

In fact, linear methods such as the Weiner filtering are the most used because of their implementation simplicity [1]. However, these methods are not sufficiently effective for transient or pulse signals.

The spectral subtraction method introduced in [2] remains an interesting choice in reducing the additive noise. Despite its capability of removing the background noise, this method introduces additional artifacts called musical noise [3].

In recent years, a non-linear approach based on wavelet transform has been proposed. The main idea is to threshold the wavelet coefficients by keeping only those which are supposed to correspond to the signal [4, 5, 6]. This method has shown a good agreement. However, a

drawback of the wavelet approach is that the analyzed functions are predetermined in advance and it is not often optimal to describe the signal non stationarity.

In the last decade, a new non linear technique, termed empirical mode decomposition (EMD), has been introduced by N. E. Huang et al. [7] for adaptively representing non stationary signals. The most important characteristic is that the basis functions are directly derived from the speech signal itself. Thus the EMD allows the decomposition of a signal into a finite sum of components, called Intrinsic Mode Functions (IMFs).

In this paper, we will present a new speech enhancement approach based essentially on the Empirical Mode Decomposition technique (EMD) and a soft thresholding approach applied on selected modes. The basic idea is to fully reconstruct the signal with all IMFs by thresholding only the first IMFs (low order components) and keeping unthresholded the last components.

2. EMPIRICAL MODE DECOMPOSITION

2.1 Principle

The principle of the EMD technique is to decompose a given signal $x(t)$ into series of oscillating components called Intrinsic Mode Functions (IMFs) via an iterative procedure called sifting process, each one with a distinct time scale. The decomposition is based on the local time scale of $x(t)$, and yields adaptive basis functions.

By mean of the EMD, the signal $x(t)$ is decomposed into fast oscillations superposed to slow oscillations. Thus, each IMF contains locally lower frequency oscillations than the one that was extracted just before.

An IMF must fulfill the two following conditions:

C1- In the whole data series, the number of local extrema and the number of zero crossings must be the same or differ at most by one.

C2- At any point, the mean value of the local maxima envelope and the local minima envelope is zero [7].

2.2 Algorithm

To determine the IMFs, denoted $imf_i(t)$, the sifting process can be summarized as follows:

1. Initialize: $r_0(t) = x(t)$, $i = 1$
2. Extract the i^{th} IMF:
 - a. Initialize: $h_0(t) = r_i(t)$, $j = 1$,
 - b. Identify the extrema (both maxima and minima) of the signal, $h_{j-1}(t)$,
 - c. Interpolate the local maxima and the local minima by a cubic spline to form upper and lower envelopes of $h_{j-1}(t)$
 - d. Compute the local mean, $m_{j-1}(t)$, by averaging the envelopes,
 - e. $h_j(t) = h_{j-1}(t) - m_{j-1}(t)$,
 if the stopping criterion is satisfied then set $imf_i(t) = h_j(t)$
 else go to (b) with $j = j + 1$
3. $r_i(t) = r_{i-1}(t) - imf_i(t)$,
4. if $r_i(t)$ still has at least two extrema then go to (2) with $i = i + 1$
 else the decomposition is finished and $r_i(t)$ is the residue.

At the end of the algorithm, the decomposition of $x(t)$ is given by:

$$x(t) = \sum_{i=1}^n \text{imf}_i(t) + r_n(t) \quad (1)$$

Where n is the mode number and $r_n(t)$ is the residue of the decomposition.

3. MODE SELECTION APPROACH

In the literature many authors have proposed approaches for signal enhancement using EMD technique based on excluding the first IMFs.

EMD extracts, sequentially and intrinsically, the energy in the signal starting from small scales (high frequency modes) towards the larger ones (low-frequency modes). The selection method is based on the assumption that the first IMFs (high-frequency modes) are mostly dominated by noise and are not representative for information specific to the original signal. Thus, the enhanced signal is reconstructed only by a few IMFs in which pure signal mostly predominates. In fact, there will be a mode, $\text{IMF}_{j_s}(t)$, from which the energy distribution of the original signal is greater than the noise. The idea is to separate signal from noise. The basic of this approach is to set to zero the first $j_s - 1$ IMFs [9]. As a result, the signal is partially reconstructed from the remaining IMFs.

Let $x(t)$ be the clean speech signal, $x_n(t)$ the noisy speech signal and $n(t)$ the noise (additive white gaussian noise). $x_n(t)$ is given as follows:

$$x_n(t) = x(t) + n(t) \quad (2)$$

The aim of this section is to find an approximation $\tilde{x}(t)$ of the original signal $x(t)$ that minimizes the mean square error (MSE) defined by [10]:

$$\text{MSE}(x, \tilde{x}) = \frac{\Delta}{N} \sum_{i=1}^N [x(t_i) - \tilde{x}(t_i)]^2 \quad (3)$$

Where $x = [x(t_1), x(t_2) \dots x(t_N)]^t$, $\tilde{x} = [\tilde{x}(t_1), \tilde{x}(t_2) \dots \tilde{x}(t_N)]^t$ and N is the signal length.

After decomposing the signal $x_n(t)$ through the EMD algorithm, $\tilde{x}(t)$ is reconstructed using $(n - j_s + 1)$ IMF indexed from j_s to n as follows:

$$\tilde{x}_{j_s}(t) = \sum_{j=j_s}^n \text{imf}_j(t) + r_n(t), j_s \in \{2, \dots, n\} \quad (4)$$

Since, the original signal $x(t)$ is unknown; the MSE cannot explicitly be calculated. That's why a distortion measure, termed consecutive MSE (CMSE) that does not require any knowledge of $x(t)$ [9] is used. The CMSE is defined as:

$$\text{CMSE}(\tilde{x}_k, \tilde{x}_{k+1}) = \frac{\Delta}{N} \sum_{i=1}^N [\tilde{x}_k(t_i) - \tilde{x}_{k+1}(t_i)]^2, \quad k \in \{1, \dots, n-1\} \quad (5)$$

$$= \frac{\Delta}{N} \sum_{i=1}^N [\text{imf}_k(t_i)]^2 \quad (6)$$

According to [10], the CMSE is reduced to the energy of the k^{th} IMF. It is also the classical empirical variance estimate of the IMF. Finally j_s is computed as:

$$j_s = \arg \min_{1 \leq k \leq n-1} [\text{CMSE}(\tilde{x}_k - \tilde{x}_{k+1})] \quad (7)$$

Where \tilde{x}_k and \tilde{x}_{k+1} are signals that are respectively reconstructed starting from the IMFs that are indexed by K and $(k+1)$.

By using the CMSE criterion, the IMF order corresponding to the first significant change in the energy distribution is identified.

4. SOFT THRESHOLDING

Many speech enhancement methods use amplitude subtraction based soft thresholding approach [5]:

$$\tilde{X} = \begin{cases} \text{sign}(X)(|X| - \tau) & \text{if } |X| > \tau \\ 0 & \text{if } |X| \leq \tau \end{cases} \quad (8)$$

Where X is the coefficient of the noisy speech signal $x_n(t)$ (as given in equation 2) obtained by the analyzing transformation, \tilde{X} is the denoised version of X and τ is the threshold parameter. According to Donoho and Johnstone in [5], a universal threshold τ is given by:

$$\tau = \tilde{\sigma} \sqrt{2 \cdot \log_e(N)} \quad (9)$$

Where N is the number of samples and $\tilde{\sigma}$ represents the noise level estimation. The expression of $\tilde{\sigma}$ is:

$$\tilde{\sigma} = \text{MAD} / 0.6745 \quad (10)$$

Here MAD represents the absolute median deviation of X .

5. PROPOSED HYBRID APPROACH

Many speech enhancement algorithms excluding the first IMFs issued from the EMD technique are revealed not efficient.

In this work, we propose a hybrid approach for speech enhancement. We don't eliminate the first IMFs but we consider them after operating a soft thresholding. The enhanced signal is constituted by the thresholded IMFs [11, 1], the remaining ones and the residue. This approach permits us to preserve the signal components in the first IMFs.

The proposed method follows four steps:

1. Decomposing a given noisy speech signal $x_n(t)$ into series of IMFs by EMD technique [7],
2. Applying on the obtained IMFs the Mode-Selection criteria to find the index j_s which minimizes the mean square error (MSE) [8],
3. Enhancing the first $(j_s - 1)$ IMFs by the soft thresholding algorithm [9] to obtain the denoised $\text{imf}_i(t)$ versions $\tilde{f}_i(t)$, $i = 1, \dots, j_s - 1$,
4. Reconstructing the enhanced following signal as follows

$$\tilde{x}(t) = \sum_{i=1}^{j_s-1} \tilde{f}_i(t) + \sum_{i=j_s}^n \text{imf}_i(t) + r_n(t) \quad (11)$$

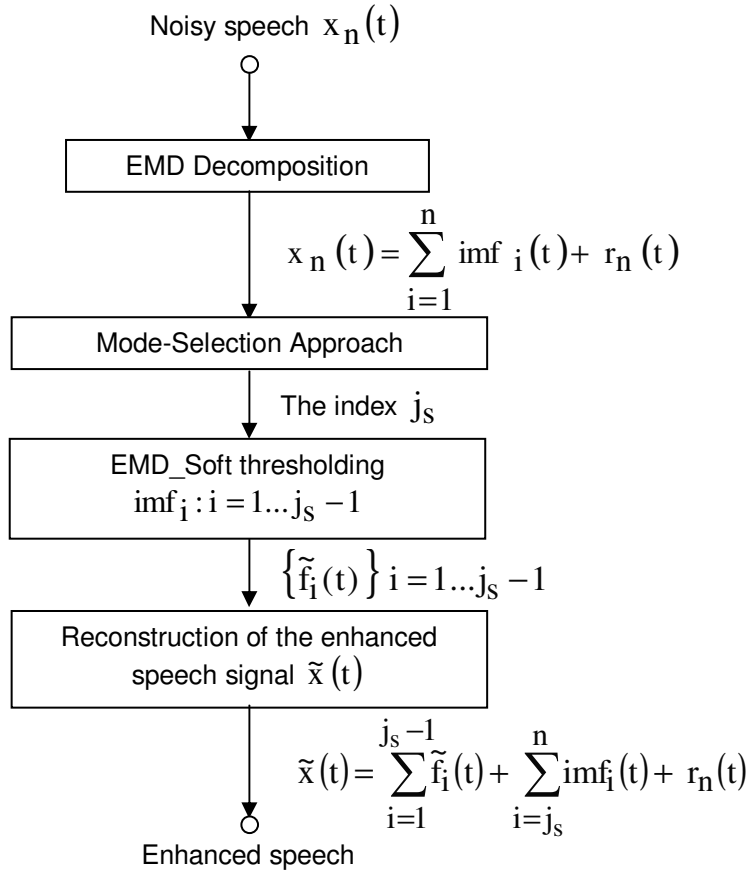


FIGURE 1: Overall block diagram of the proposed method for speech enhancement.

6. RESULTS

In order to illustrate the effectiveness of our proposed method, a total of ten sentences (5 male and 5 female speakers) taken from the NOISEUS database are used in our evaluation. The analysis is conducted by adding to the clean speech signal a white Gaussian noise with various SNR levels -5, 0, +5 and +10 dB. To operate an objective performance evaluation of our speech enhancement approach, both output SNR and Weighted Spectral Slope (WSS) distance proposed in [12], are computed.

Figure 2 illustrates the original clean speech signal taken from the NOISEUS database and pronounced by the speaker sp03 followed by the same speech signal corrupted by an additive white Gaussian noise with an input SNR of 5dB. The last signal shows the enhanced speech signal using our approach. It can be observed that the noise is reduced in the enhanced speech signal and has a shape very close to the corresponding clean speech.

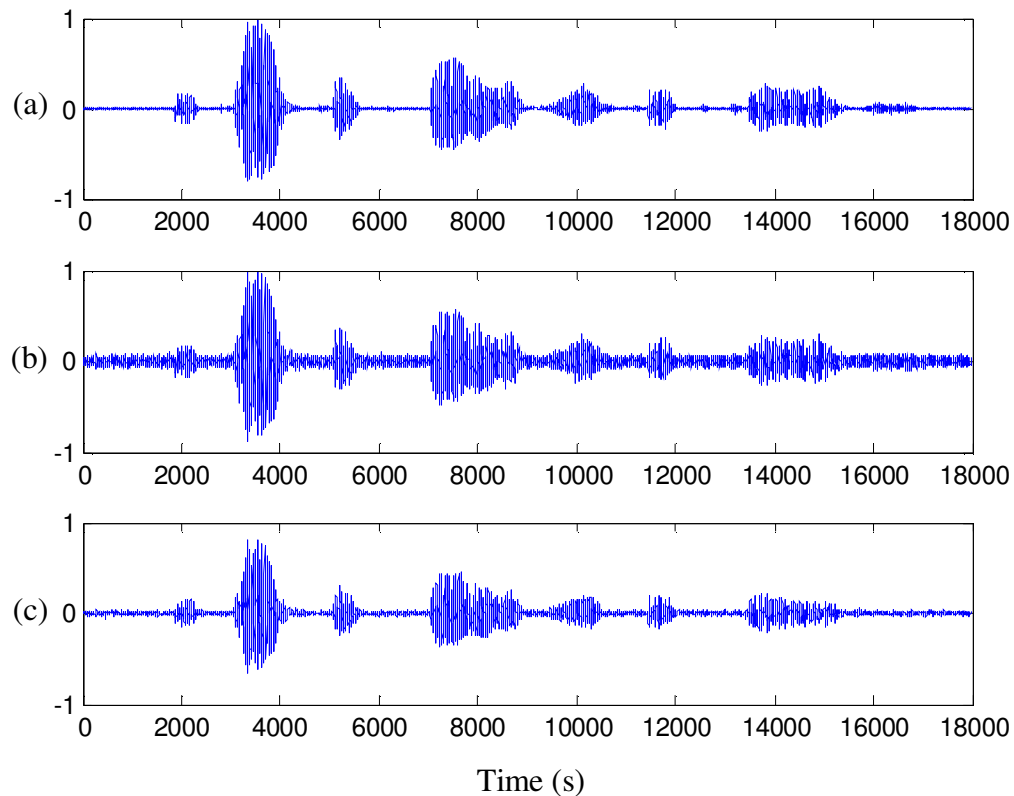


FIGURE 2: Waveform of the clean speech (a), the noisy speech at SNR of 5dB (b) and the enhanced speech signal with our proposed method (c).

In our evaluation, we compare our proposed method to two approaches using EMD soft thresholding of all IMFs and the elimination of the first IMFs [10]. We use two criterions:

- The output SNR of the enhanced speech signal.

Input SNR (dB)	Output SNR (dB)		
	First IMFs elimination	EMD_soft	Proposed
-5	0,290	0,583	0,387
0	1,090	1,211	1,474
5	3,683	4,379	6,094
10	8,449	8,719	13,058

TABLE 1: Comparison of the output SNR levels for various denoising methods.

- The Weighted Spectral Slope (WSS) measure:

The measure is based on the auditory model in which 36 overlapping filters of progressive larger bandwidth are used to estimate the smoothed short-time speech spectrum [12]. The measure finds a weighted difference between the spectral slopes in each band. The magnitude of each weight reflects whether the band is near a spectral peak or valley, and whether the peak is the largest in the spectrum. A per-frame measure in decibels is found as:

$$d_{wss}(j) = K_{SPL}(K - \hat{K}) + \sum_{k=1}^{36} w_a(k)[x(k) - \hat{x}(k)]^2 \quad (12)$$

Where $(K - \hat{K})$ is the difference between overall sound pressure level of the original and processed utterances. K_{SPL} is a parameter which can be varied to increase the overall performances.

Input SNR (dB)	d_{wss}		
	First IMFs elimination	EMD_soft	Proposed
-5	105,157	122,557	104,997
0	75,924	124,531	79,438
5	66,167	104,320	60,394
10	46,235	72,143	35,974

TABLE 2: Comparison of the WSS measure for various denoising methods.

Referring to tables 1 and 2, one can clearly notice the following interpretations:

- Table 1 depicts the SNR of the enhanced speech signal compared to the SNR at the input. The proposed approach improves the speech quality by reducing the noise and performing better than the other methods at SNRs of 0, +5 and +10 dB.

- Table 2 shows the WSS evaluation criteria for our approach and two others. Our approach gives the less WSS distance for almost all the SNR levels showing its convenience for speech enhancement.

- The Mode Selection approach proposed by Boudraa in [10] is effective especially for very noisy signals. For this reason, the increase of the input SNR level leads to lower values of output SNR. This decrease is logical because on one hand this approach eliminates the first IMFs and on the other hand, for high values of input SNR, we tend toward the original signal. This causes the degradation of the original signal, and hence the interest of our approach whose principle is to keep all IMFs. As shown by Cexus and Boudraa in [11], the EMD soft thresholding performs almost better than the soft thresholding using Wavelet transform, what justifies the enhancement of the first IMFs by EMD soft thresholding applied in our work.

7. CONCLUSION

In this paper, we propose a new approach based on EMD technique for speech enhancement. It consists of four essential steps:

- The first step concerns the empirical mode decomposition of the noisy speech signal.
- The second step concerns the index mode selection j_s using an energy criterion.
- The third step concerns the soft thresholding of the first $j_s - 1$ IMFs.
- And the fourth step concerns the signal reconstruction by adding the thresholded IMFs, the remaining IMFs and the residue.

This approach shows efficiency when compared to other approaches based also on EMD technique.

8. REFERENCES

- [1] A.O. Boudraa and J.C. Cexus, "Denoising via empirical mode decomposition," in Proc. IEEE ISCCSP, Marrakech Morocco, 2006.
- [2] S. F. Boll, "Suppression of acoustic noise in speech using spectral subtraction," IEEE Transactions on Acoustics Speech and Signal Processing, ASSP-27 pp. 113-120, 1979
- [3] A. Sumithra M G , B. Thanuskodi K, C. Anitha M R, "Modified Time Adaptive Wavelet Based Approach for Enhancing Speech from Adverse Noisy Environments," DSP Journal, Volume 9, Issue 1, p.p. 33-40, June, 2009
- [4] D.L. Donoho, "De-noising by soft-thresholding," IEEE Trans. on Information Theory, 41(3):613–627, 1995.
- [5] D.L. Donoho and I.M. Johnstone, "Ideal spatial adaptation via wavelet shrinkage," Biometrika, vol. 81, pp. 425–455, 1994.
- [6] S. Mallat, "Une Exploration Des Signaux En Ondelettes," Ellipses, Paris, France, 2000.
- [7] N. E. Huang, Z. Shen, S. R. Long, M. C. Wu, H. H. Shin, Q. Zheng, N. C. Yen, C. C. Tung, and H. H. Liu, "The empirical mode decomposition and the Hilbert spectrum for nonlinear and non-stationary time series analysis," Proc. R. Soc. Lond. A, Math. Phys. Sci., Mar. 1998, vol. 454, no. 1971, pp. 903–995.
- [8] E. Dergler, Md. K. I. Molla, M. Hirose, N. Minematsu, and Md. K. Hasan, "Speech Enhancement using Soft Thresholding with DCT-EMD Based Hybrid algorithm," Proc. EUSIPCO-2007, Poznań, POLAND, 2007, pp. 75–79.
- [9] J.C. Cexus, "Analyse des signaux non-stationnaires par Transformation de Huang, Opérateur de Teager-Kaiser, et Transformation de Huang-Teager (THT)," Thesis, Université de Rennes 1, 2005.
- [10] A. O. Boudraa, and J.C. Cexus, "EMD-Based Signal Filtering," IEEE Trans. On Instrumentation and measurement, vol. 56, no. 6, pp. 2196–2202, December 2007.
- [11] A.O. Boudraa, J.C. Cexus, and Z. Saidi, "EMD-based signal noise reduction," Int. J. Sig. Process., vol. 1, no. 1, pp. 33–37, 2004, ISSN: 1304-4494.
- [12] D. H. Klatt, "Prediction of Perceived Phonetic Distance from Critical-Band Spectra: A First Step," Proc. IEEE ICASSP'82, May, 1982, Vol. 2, pp. 1278-1281.

Classification of Cardiac Arrhythmia Using WT, HRV, and Fuzzy C-Means Clustering

A. Dallali

*Fac Sc University of Gafsa
Gafsa, 2100, Tunisia*

adel.dallali@gmail.com

A. Kachouri

*ENIS/LETI University of Sfax
Sfax, 3400, Tunisia*

Kachouri.abdenaceur@enis.rnu.tn

M. Samet

*ENIS/LETI University of Sfax
Sfax, 3400, Tunisia*

Mounir.samet@enis.rnu.tn

Abstract

The classification of the electrocardiogram registration into different pathologies disease devises is a complex pattern recognition task. In this paper, we propose a generic feature extraction for classification of ECG arrhythmias using a fuzzy c-means (FCM) clustering and Heart Rate variability (HRV). The traditional methods of diagnosis and classification present some inconveniences; seen that the precision of credit note one diagnosis exact depends on the cardiologist experience and the rate concentration. Due to the high mortality rate of heart diseases, early detection and precise discrimination of ECG arrhythmia is essential for the treatment of patients. During the recording of ECG signal, different forms of noise can be superimposed in the useful signal. The pre-treatment of ECG imposes the suppression of these perturbation signals. The row date is preprocessed, normalized and then data points are clustered using FCM technique.

In this work, four different structures, FCM-HRV, PCM-HRV, FCMC-HRV and FPCM-HRV are formed by using heart rate variability technique and fuzzy c-means clustering. In addition, FCM-HRV is the new method proposed for classification of ECG.

This paper presents a comparative study of the classification accuracy of ECG signals by using these four structures for computationally efficient diagnosis. The ECG signals taken from MIT-BIH ECG database are used in training to classify 4 different arrhythmias (Atrial Fibrillation Termination).

All of the structures are tested by using the same ECG records. The test results suggest that FCMC-HRV structure can generalize better and is faster than the other structures.

Keywords: Fuzzy C-Means Clustering, WT, HRV, Arrhythmia, MCN, Classification.

1. INTRODUCTION

Electrocardiography deals with the electrical activity of the central of the blood circulatory system, i. e. the heart. Monitored by placing sensors at the limb extremities of the subject, electrocardiogram (ECG) is a record of the origin and the propagation of the electrical potential through cardiac muscles [1]. Thus, ECG is an important non – invasive clinical tool for the diagnosis of heart diseases [2].

The state of cardiac heart is generally reflected in the shape of ECG waveform and heart rate. It may contain important pointers to the nature of diseases afflicting the heart. Early and quick detection and classification of ECG arrhythmia are important, especially for the treatment of patients in the intensive care unit. In recent years, computer assisted ECG interpretation and automatic classification has received great attention from the biomedical engineering community.

This is mainly due to the fact that ECG signal provides cardiologists with useful and important information concerning the dysfunctions and physical condition of human heart. In designing of CAI system, the most important is the integration of suitable features extractor and pattern classifier such that they can operate in coordination to make an effective and efficient system [2]. Several algorithms have been developed in the literature for detection and classification of ECG records. One of the methods of ECG beat recognition is neural network classification method (dallali ssd'03; engine & demirag 2003; foo, stuart & meyer – baese 2002).

The hybrid system of neural network and fuzzy logic has been widely accepted for pattern recognition tasks (Mean et al2 2006; ozbay, ceylam, & karlik 2006). Yu et al. have implemented the integration of independent component analysis and neural network classifier (ICA – NN) along with R-R intervals to discriminate eight types of ECG beats [3].

In [3, 4], Ozbay et al. had combined principal component analysis with neural network (PCA –NN) and compared with wavelet transform technique for ECG signal classification. In [5], T.M. Nazmy had combined ICA and hybrid system (ICA –ANFIS) for ECG signal classification. In this paper, we evaluate the integration of WT-FCM to discriminate four types of ECG beats. The proposed structure is composed of three sub - systems: the filtrate, wavelet transform to extract the parameters, and classification by FCM technique.

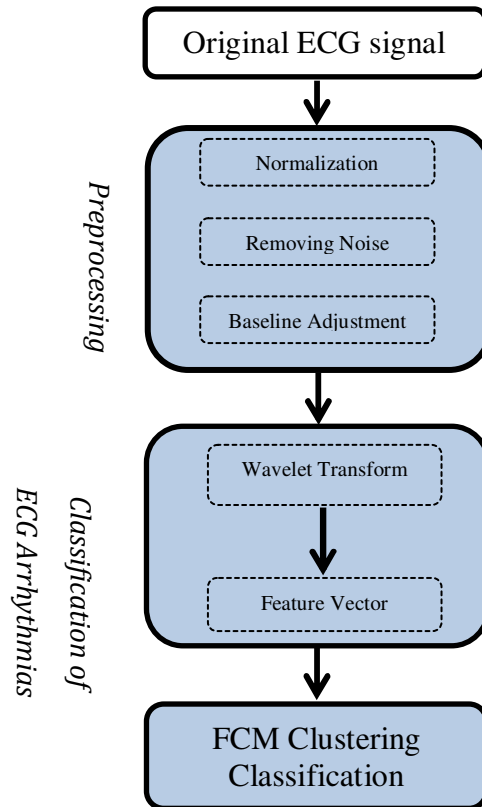


FIGURE 1: Block diagram of proposed arrhythmia classifier

Figure 1 summarizes the classification steps of the signals. One distinguishes the stage of data Conditioning (sampling and filtering), the stage of extraction of the characteristics and the stage of FCM algorithm (training of the data and validation of the test data).

All the samples must be normalized in order to have the features at the same level. ECG signals can be contaminated with several kinds of noise, such as power line interference (A/C), baseline wandering (BW), and electromyography noise (EMG), which can affect the extraction of parameters used for classification, so we want to filter the signal. The unwanted noise of the signal must be removed. ECG were filtered using Low pass filter, high pass filter. The pre-

treatment of ECG signals imposes the suppression of each perturbation signals, the noise high frequency electromyography and the low frequency drift. After that, the signal baseline may be shifted from zero line. The baseline of the ECG signal was adjusted at zero line by subtracting the median of the ECG signal [8, 9].

2. CHARACTERISTICS OF THE ECG

The ECG represents the wave's electrical propagation through the respective regions of the heart (SA. node, Atrial Muscle, AV node, Atria ventricular Bundle, Left and Right Bundle Branches). These waves are the major evident observable of the human heart and have been used to intensive diagnosis since of their significance in the context of pathologies [11].

Usually, the listing of the electrical wave's variations on the papers constitutes the ECG signal.

Figure 1 shows the temporal characteristics of normal ECG.

Mechanical actions	associated Wave	Duration (sec)	Amplitude (mV)	wave Frequency (Hz)	Axe
Auricular depolarization	P wave	<0.12	≤ 0.3	10	20° à 80°
Depolarization of the ventricle	QRS Complex	0.08 à 0.12	Q<0 - S>0 R (0.5-2) DI + DII+ DIII > 15	20 - 50	-30° à +110° < -30° axe gauche > 110° axe droit
Repolarization of the ventricles	T wave	0.2	0.2	5	
Repolarization of the auricles	Hidden wave				

TABLE 1: ECG properties

3. REVIEW OF LITERATURE

CUIWEI Li et al., (1995) showed that it is easy with multi scale information / decomposition in wavelets transformation to characterize the ECG waves. KHADRA et al. (1997) proposed a classification of life threatening cardiac arrhythmias using wavelet transforms. MG Tsipouras and al (2004) used time frequency analysis for classification of atrial tachyarrhythmia. Mei Jiang Kong and al. (2005) used block-based neural networks to classify ECG Signals. Srinivasca K G, Amrinder Singh, A O Thomas, Venugopal K R and L M Patnaik, (2005) used Fuzzy C – Means Clustering for classification of generic feature extraction. (2007), Ceylan, R. & Ozbay, Y. proposed a classification of ECG arrhythmias using neural network method based in techniques of FCM, PCA and WT.

4. MATERIALS AND METHODS

In many pattern recognition applications, the task of partitioning a pattern set can be considered to be the result of clustering algorithms in which the cluster prototypes are estimated from the information of the pattern set. In many cases, it may be impossible to obtain exact knowledge from a given pattern set. For recognition of the ECG arrhythmias, different methods were presented in the literature, such as the MLP approach, LVQ. In this paper, we present the combination of different forms of fuzzy c-means clustering, and wavelet transform; named as WT – FCM or HRV – FCM and then compare this technique with the other models of FCM.

4.1 Wavelet Transform

The ECG signals are considered as representative signals of cardiac physiology, which are useful in diagnosing cardiac disorders. The WT provides very general and power full techniques, which can be applied to many tasks in signal processing. The most important application is the ability to compute and manipulate data in compressed parameters. Thus, the ECG records can be compressed into a few useful parameters. These parameters can be used for recognition and

diagnosis. Selection of appropriate wavelet and the level of decomposition is very important in treatment of signals using WT. the smoothing feature of the Daubechies wavelet of order 3 made it more suitable to detect variation on the ECG signals [8]. Therefore, the wavelet coefficients were computed using the Daubechies wavelet of level 3 in the present work.

4.2 The fuzzy C-means Clustering

The FCM algorithm has successfully been applied to a wide variety of clustering problems. The FCM algorithm attempts to partition a finite collection of elements $X = \{x_1, x_2, \dots, x_N\} \subset R^h$ where N represents the number of data vectors and h the dimension of each data vector, into a collection of C fuzzy clusters. C – Partition of X constitutes sets of $(c.N)$ $\{u_{ij}\}$ member ship values can be conveniently arranged as a $(c.N)$ matrix $u = [u_{ij}]$. The objective of fuzzy clustering is to find the optimum member ship matrix U . the most widely used objective function for fuzzy clustering is the weight within – groups sum of squared errors J_m , which is used to define the following constrained optimization problem [13].

$$J_m = \sum_{i=1}^N \sum_{j=1}^c u_{ij}^m \|x_i - c_j\|^2 \quad (1)$$

Where $1 \leq m < \infty$, i. e. m is any real number greater than 1, u_{ij} is the degree of member ship of x_i in the cluster j , x_i is the i th component of d -dimensional measured data, c_j is the d – dimension center of the cluster, and $\| \cdot \|$ is any norm expressing the similarity between any measured data and the center. Fuzzy partition is carried out through an iterative optimization of the objective function shown above, with the update of member ship u_{ij} .

$$u_{ij} = \frac{1}{\sum_{k=1}^c \left(\frac{\|x_i - c_{ij}\|}{\|x_i - c_{jk}\|} \right)^{\frac{2}{m-1}}} \quad (2)$$

and the cluster c_j by:

$$c_j = \frac{\sum_{i=1}^N u_{ij}^m \cdot x_i}{\sum_{i=1}^N u_{ij}^m} \quad (3)$$

This iteration will stop when error $\|u_{ij}^{k+1} - u_{ij}^k\| \leq \epsilon$, where ϵ is a termination criterion between 0 and 1; whereas k are the iteration steps. This procedure converges to a local minimum or a saddle point of J_m . The algorithm is composed of the following steps:

The steps are as follows:

- i- Initialize the number of clusters (c), weighting exponent (m), iteration limit, termination criterion ($\epsilon > 0$) and $U=[u_{ij}]$ matrix, $U(0)$.
- ii- Guess initial position of cluster centers.
- iii- At k step calculate the center vectors $c^k = [c_j]$

$$c_j = \frac{\sum_{i=1}^N u_{ij}^m x_i}{\sum_{i=1}^N u_{ij}^m}$$

- iv- Update $U(k)$ to $U(k+1)$

$$u_{ij} = \frac{1}{\sum_{k=1}^c \left(\frac{\|x_i - c_j\|}{\|x_i - c_k\|} \right)^{\frac{2}{m-1}}}$$

If $\|U^{(k+1)} - U^{(k)}\| \leq \epsilon$ then stop; otherwise to step (i)

5. PROPOSED METHOD

The method is divided into four steps: (i) ECG sampling and processing, (ii) data reduction, (iii) extraction of feature vector, and (iv) classification using FCM clustering. The validation of the proposed algorithm for the HRV extraction is done using 80 original ECG record of ECG data base [17]. The ECG signals used in this work are obtained from MIT – BIH arrhythmia database. The sampling frequency is 360 Hz in different classes. A total of 152 samples HRV attributing to four ECG beat types are summarized in table 1, in which half of the ECG beats are selected for training and the other half for testing the classification

Type	MIT – BIH data base	Training file	Testing file
1	n01, n02, n03, n04	20	18
2	S01, s02, s03, s04	20	18
3	A01, a02, a03, a04	20	18
4	B01, b02, b03, b04	20	18
Total		80	72

TABLE 2: ECG samples used in this study

The associated RR interval is calculated from the location of the R points documented in the annotation files of the MIT – BIH database

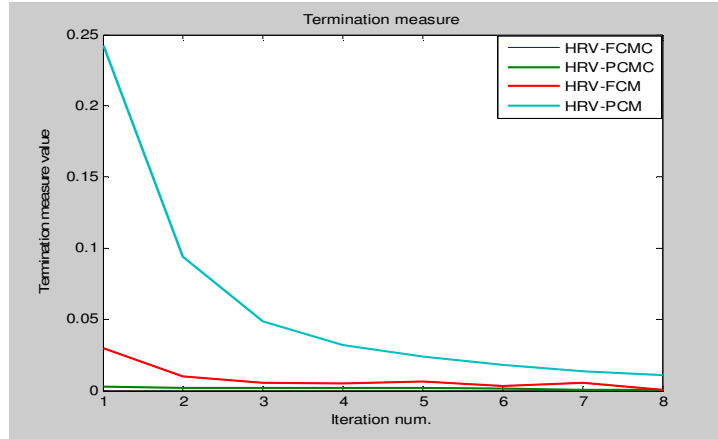


FIGURE 2: Convergence performance of different structure of FCM

Figure 2 shown that FCMC and PCMC have the same graph. PCMC is applied to noisy signals. So, FCMC is widely applied in this work as the signals are filtered before use.

Arrhythmia types of test pattern	Number of beats	FCMC		FCM		PCM		PCMC	
		MCN	RMC (%)	MC N	RMC (%)	MCN	RMC (%)	MCN	RMC (%)
1	20	0	0	1	5	0	0	0	0
2	20	0	0	0	0	0	0	1	5
3	20	0	0	2	10	2	10	0	0
4	20	1	5	0	0	2	10	0	0
Total	80	1	1.25	3	3.75	4	5	1	1.25
Average test error (%)		0.0118		0.0126		3.026		0.0118	

TABLE 3: pre – classification results for each arrhythmia in test

6. TEST RESULTS

Table 3 describes the test errors for each arrhythmia obtained with FCM and the other three structures. Misclassification Number (MCN) noted in table 3 represents number of misclassification ECG in testing. Rate of misclassification (RMC) is calculated using:

$$RMC (\%) = \left(\frac{\text{Number of misclassification beat}}{\text{Number of total beat}} \right) \quad (4)$$

The performance of FCMC – HRV technique is depicted as shown in figure 1. It is observed that the % of error in case of WT – FCMC allows us to make a comparison to others structures keeping the number of the same iteration

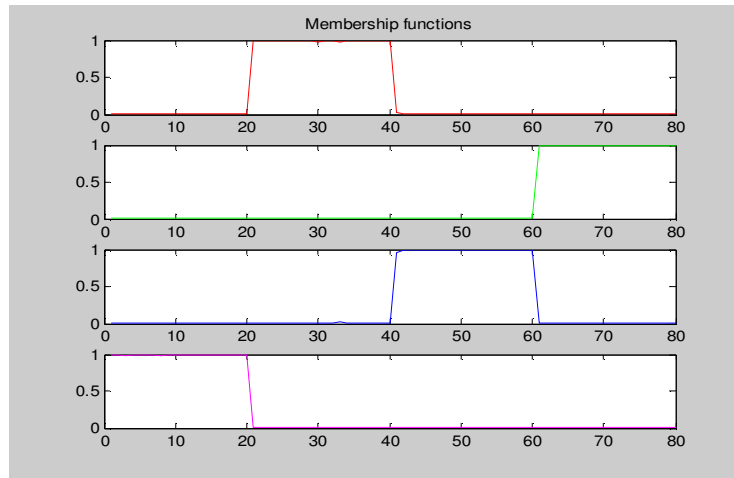


FIGURE 3: Classification results for different classes

Figure 3 shows the output of the FCM classifier. All the ECG arrhythmias detected from the ECG records are classified correctly. As noted, recognition rates vary between 98.5 and 99.6 with average accuracy 99.05

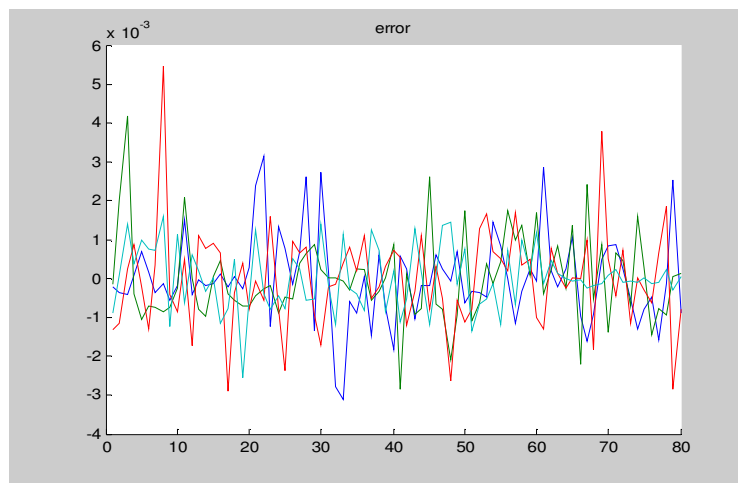


FIGURE 4: Error of classification for different classes

The error curve (figure 4), illustrates the smallest values obtained for the classification of different arrhythmias (less than 0.6 %).

7. CONCLUSION

For the conventional FCMC, all patterns in the pattern space are assigned membership values, which are based on the Enclidean distance between the patterns to each cluster.

This paper represents new method for the classification of ECG arrhythmia signal using Fuzzy C-Means algorithm. The method has been comprehensively tested using the ECG database covering wide variety of ECG arrhythmias. In this paper, the WT – FCMC has been developed and presented to classify electrocardiography signals. In doing so, a comparative assessment of the performance of FCM shows that more reliable results are obtained with the FCMC in shorter time for the classification of ECG signals. The aim in developing WT – FCM was to achieve more optimum cluster centers locations and to reduce the time of training of the structure. We hope that

the performance of the method will be better if we use a neural network to classify the output of the FCM clusters (WT-FCM-NN).

This technique is obtained by incorporating the technique preprocessing different ECG signal, fuzzy c-means clustering method for classification of ECG arrhythmias. So, it can be said that the structure, which is a widely beneficial structure than conventional WT – NN to recognize and classify ECG signals, is obtained.

8. REFERENCES

Article in a Journal

- [1] Owis, M. I., Youssef, A.-B. M., & Kadah, Y. M., "Characterization of ECG signals based on blind source separation," *Medical and Biological Engineering and Computing*, vol. 40, pp. 557–564, 2002.
- [2] Rahime Ceylan a,* , Yuksel Ozbay a, Bekir Karlik b, 2009. A novel approach for classification of ECG arrhythmias: Type-2 fuzzy clustering neural network. *Expert Systems with Applications*,6721-6726
- [3] Yu, S.-N., & Chou, K.-T., "Integration of independent component analysis and neural networks for ECG beat classification," *Expert Systems with Applications*, vol. 34, pp. 2841-2846, 2008.
- [4] Ceylan, R., & Ozbay, Y. (2007). Comparison of FCM, PCA and WT techniques for classification ECG arrhythmias using artificial neural network. *Expert Systems with Applications*, 33, 286–295.
- [5] Guler, I. & Ubeyli, E. D., "ECG beat classifier designed by combined neural network model," *Pattern Recognition*, vol. 38, pp. 199-208, 2005.
- [6] M. I. Owis, A. B. M. Youssef and Y. M. Kadah. "Characterisation of electrocardiogram signals based on blind source separation" ,*Medical & Biological Engineering & Computing*, Cairo, Egypt 2002.
- [7] Dipti Patra and Smita Pradhan, "Integration of FCM, PCA and Neural networks for classification of ECG Arrhythmias," *IAENG International Journal of Computer Science*, 36:3, IJCS_36_3_05 , 01 August. 2009.
- [8] E. M. Tamil, N. H. Kamarudin, R. Salleh, M. Yamani Idna Idris, M. N. Noorzaily, and A. M. Tamil, (2008) Heartbeat electrocardiogram (ECG) signal feature extraction using discrete wavelet transforms (DWT), in *Proceedings of CSPA*, 1112–1117
- [9] A. Dallali, A. Kachouri, and M. Samet, "A Comparison of Wavelets_Based to Guaranteeing ECG Compression quality". *World Academy of Science, Engineering and Technology* 55 2009
- [10] Yu, S.-N., & Chou, K.-T., "Integration of independent component analysis and neural networks for ECG beat classification," *Expert Systems with Applications*, vol. 34, pp. 2841-2846, 2008.
- [11] Srinivasca K G, Amrinder Singh, A O Thomas, Venugopal K R and L M Patnaik," Generic Feature Extraction for Classification using Fuzzy C – Means Clustering", 0- 7803 – 9588 – 3/05/\$20.00 ©2005 IEEE.
- [12] A. Kachouri, M. Ben Messaoud and A. Dallali: 'Wavelet based on Electrocardiogram Signal Analysis for Classification and Diabnosis By Neural Networks', *SSD'03 March 26-28, 2003 – Sousse, Tunisia*

- [13] Yu, S. N., & Chen, Y. H. (2007). Electrocardiogram beat classification based on wavelet transformation and probabilistic neural network. *Pattern Recognition Letters*, 28, 1142–1150.
- [14] B. Anuradha and V.C. Veera Reddy June 2008. ANN For Classification Of Cardiac Arrhythmias. *ARPN Journal of Engineering and Applied Sciences*. Vol. 3, NO. 3, June 2008
- [15] B.U. Kohler, C. Hennig and R. Orglmeister, "The principles of software QRS detection", *IEEE Engineering in Medicine and Biology Magazine*, vol. 21, no. 1, pp. 42-57, Jan.-Feb. 2002.
- [16] S. Z. Mahmoodabadi, A. Ahmadian, and M. D. Abolhasani, "ECG Feature Extraction using Daubechies Wavelets", *Proceedings of the fifth IASTED International conference on Visualization, Imaging and Image Processing*, pp. 343-348, 2005.

Electronic References

- [17] <http://www.physionet.org/physiobank/database/mitdb/>
- [18] <http://www.physionet.org/physiobank/database/slpdb/>

Power Efficiency Improvement in CE-OFDM System With 0 dB IBO for Transmission over PLC Network

El Ghzaoui Mohammed

*Laboratory of Transmission and Data processing,
University Sidi Mohammed Ben Abdellah,
Fez, morocco*

elghzaoui.mohammed@gmail.com

Belkaidid Jamal

*Laboratory of Transmission and Data processing,
University Sidi Mohammed Ben Abdellah,
Fez, morocco*

belkaidid@gmail.com

Benbassou Ali

*Laboratory of Transmission and Data processing,
University sidi Mohammed ben Abdellah,
Fez, morocco.*

alibenbassou@gmail.com

EL Bekkali Moulhim

*Laboratory of Transmission and Data processing,
University sidi Mohammed ben Abdellah,
Fez, morocco*

bekkali@gmail.com

Abstract

Orthogonal frequency division multiplexing (OFDM) OFDM has been adopted for high speed data transmission of multimedia traffic such as HomePlug A/V and Mobile WiMax. However, OFDM also has a drawback of a high PAPR (peak-to-average-power-ratio). Due to this high PAPR amplifier usually does not act in dynamic range. One potential solution for reducing the peak-to-average power ratio (PAPR) in an OFDM system is to utilize a constant envelope OFDM (CE-OFDM) system. Furthermore, by utilizing continuous phase modulation (CPM) in a CE-OFDM system, the PAPR can be effectively reduced to 0 dB, allowing for the signal to be amplified with a power efficient non-linear power amplifier with Input Back-Off (IBO) of 0 dB. This paper describes a CE-OFDM based modem for Power Line Communications (PLC) over the low voltage distribution network. Relying on a preliminary characterization of a PLC network, a complete description of the modem is given. Also CE-OFDM is compared with conventional OFDM under HomePlug 1.0 in the presence of power amplifier nonlinearities, considering different values of IBO.

Key words: OFDM, CE-OFDM, PAPR, IBO, PLC, BER.

1. INTRODUCTION

Indoor power line channels are frequency and time selective, with remarkable disparity even among different locations in a specific site. The frequency selective characteristics of indoor power line channels in the frequency band up to 30 MHz have been reported in [1, 2]. Recent studies have extended the analysis up to 100 MHz [3]. Time variations have a twofold nature: long-term changes caused by the connection and disconnection of electrical appliances and periodic short-term changes, synchronous with the mains, due to the time-variant behavior of the impedance and the noise emitted by the electrical devices. Regarding the noise, it is composed of the following terms: colored background noise, impulsive components and narrowband interferences [4].

The orthogonal frequency division multiplexing (OFDM) transmission scheme is suitable for frequency-selective channels because of its ability to cope with this feature by dividing the

available bandwidth into N equally spaced narrowband sub-channels [5, 6, 7]. A data stream is distributed to subcarriers (each subcarrier is centred in one sub-channel) and transmitted in parallel. OFDM has two primary drawbacks: The first is a high sensitivity to time variations in the channel caused by Doppler, carrier frequency offsets, and phase noise. The second is that the OFDM waveform has high amplitude fluctuations, a drawback known as the (PAPR) problem. Without sufficient power back-off, the system suffers from spectral broadening, inter-modulation distortion, and, consequently, performance degradation. . There are several techniques for PAR reduction in OFDM systems has been proposed in literature [8, 9, 10].

Constant Envelope OFDM (CE-OFDM) provides one solution to the high PAPR issue in OFDM [11, 12, 13]. The idea of constant envelope OFDM with phase modulation (OFDM-PM) system was introduced. In [14] an approach is presented which transforms the high PAPR OFDM waveform into a 0 dB PAPR CE-OFDM-based waveform called OFDM phase modulation. The significance of the 0 dB PAPR achieved by using phase modulation (PM) is that the signal can be amplified with power efficient nonlinear power amplifier. Although the CPM has low spectral efficiency, it features low system complexity and favorable performance due to low PAR and robustness to amplitude variation and impulsive noise [15], which causes bit errors in data transmission, due to connected electrical appliances such as transformers, industrial switches etc. in the PLC network. The CPM decreases the side lobe of the power spectrum by means of continuously connecting the phase that contains the information. The CE-OFDM-CPM approach described in this paper is based on the phase modulator transform technique. In essence, the OFDM waveform is used to phase modulate the carrier. The OFDM-PM signal can be viewed as a type of digital FM, whereby the modulating phase signal is a real-valued OFDM baseband waveform. In this paper a CE-OFDM modulation will be introduced in order to create a complete picture of PLC channel. Our simulation model is based on the measurements in the real PLC transmission environment.

The paper is organized as follows. In section (2 and 3), we propose a detailed description of the transmitter and the receiver. In section 4, Measurement and simulation results are shown, the effect of load impedance on the Bit Error Rate (BER) performance is investigated. CE-OFDM-CPM is then compared with conventional OFDM under *homeplug 1.0* in the presence of nonlinear power amplification. The effect of the modulation index and modulation order on the BER performance is investigated.

2. CE-OFDM-CPM SIGNAL DESCRIPTION

Consider the baseband OFDM waveform:

$$m(t) = \sum_t \sum_{k=1}^N I_{i,k} q_k(t - iT_B) \quad (1)$$

Where $\{I_{i,k}\}$ are the data symbols and $\{q_k(t)\}$ are the orthogonal subcarriers.

The CE-OFDM signal is obtained through a simple transformation of OFDM. The OFDM signal is phase modulated onto a carrier signal to obtain a constant envelope signal with 0dB PAPR. This is implemented through a straight forward modification of a standard OFDM system as shown in Figure 1.

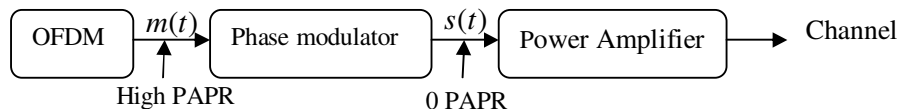


FIGURE 1: The modification of an OFDM system to obtain CE-OFDM

The baseband CE-OFDM signal is,

$$s(t) = Ae^{j\theta(t)} \quad (2)$$

Where A is the signal amplitude. The phase signal $\phi(t)$ with the embedded OFDM signal is given as:

$$\phi(t) = \theta_i + 2\pi h c_N \sum_{k=1}^N I_{i,k} q_k(t - iT_B), \quad iT_B \leq t < (i+1)T_B \quad (3)$$

Where $\theta(t) = \phi(iT - \varepsilon) - \phi(iT + \varepsilon), \quad \varepsilon \rightarrow 0$

The real data symbols $I_{n,k}$ modulate the orthogonal OFDM subcarriers $q_k(t)$. The phase memory θ_i may be used in conjunction with a phase unwrapper at the receiver to ensure a continuous phase at the symbol boundaries and hence better spectral containment [15]. Here h refers to modulation index; N is the number of sub-carriers. The normalizing constant, c_N , is set to where σ_I is the variance of the data symbols, and consequently the variance of the phase $c_N = \sqrt{\frac{2}{N\sigma_I^2}}$ signal will be $\sigma_\phi^2 = (2\pi h)^2$. Assuming that the data is independent and identically distributed, it follows that $\sigma_I^2 = \frac{M^2 - 1}{3}$.

The signal energy E_s and the bite energy E_b are

$$E_s = A^2 T_B, \quad E_b = \frac{E_s}{N \log_2(M)} \quad (4)$$

To guarantee continuous phase, the memory terms set to

$$\theta_i = K \sum_{l=0}^{\infty} \sum_{k=1}^N [I_{i-l,k} A_b(k) - I_{i-1-l,k} A_e(k)] \quad (5)$$

Where $K = 2\pi h c_N, \quad A_b(k) = q_k(0), \quad A_e(k) = q_k(T_B - \varepsilon), \quad \varepsilon \rightarrow 0$.

The benefit of continuous phase CE-OFDM is a more compact signal Spectrum. The CPM decreases the side lobe of the power spectrum by means of continuously connecting the phase that contains the information. CPM features low system complexity and favorable performance due to low PAR and robustness to amplitude variation and impulsive noise [16].

3. PM RECEIVER

A practical receiver such as the PM receiver can be used for CE-OFDM. It consists of a phase demodulator to undo the transformation followed by a standard OFDM demodulator as shown in Figure 2. Although this results in a sub-optimum receiver, it provides for a simple and practical receiver implementation.

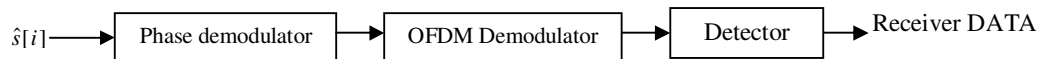


FIGURE 2: The modification of a standard OFDM receiver to obtain a CE-OFDM receiver

The CE-OFDM-CPM is a modulation format that can be viewed as a mapping of the OFDM signal onto the unit circle. The resulting signal has a constant envelope leading to a 0 dB PAPR. The OFDM signal is transformed through continuous phase modulator to a low-PAPR signal prior to the PA and at the receiver, the inverse transform by a phase demodulator is performed prior to OFDM demodulation as shown in Figure 3. The phase demodulator receiver is a practical implementation of the CE-OFDM-CPM receiver and is therefore of practical interest. However, it isn't necessarily optimum, since the optimum receiver is a bank of MN matched filters one for each potentially transmitted signal.

The phase demodulator receiver essentially consists of a phase demodulator followed by a conventional OFDM demodulator. The received signal is first passed through a front-end band pass filter, which limits the bandwidth of the additive noise [14]. An $\arg(\cdot)$ operation to calculate the phase of the received samples, and a phase unwrapper to eliminate of phase ambiguities. This receiver is shown to be insensitive to phase shifts caused by the channel. It is shown that with the introduction of memory, CE-OFDM is made phase-continuous and,

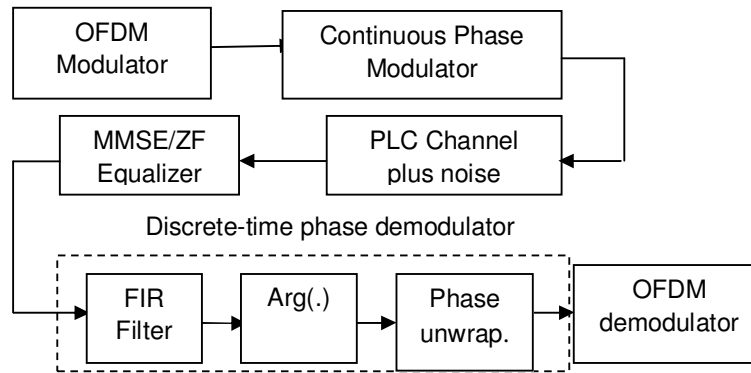


FIGURE 3: CE-OFDM-CPM block diagram

consequently, has a more compact spectrum. An additional bonus of the non-coherent receiver is it demodulates continuous phase CE-OFDM signals with no added complexity.

4. MEASUREMENT AND SIMULATION RESULTS

4.1. Measurement Results

We have made frequency response measurements for in-building power line channels in the frequency range of (1–100 MHz). As can be seen in figure 5, the frequency response exhibits considerable frequency dependent variation, due to the specific wiring configurations encountered. The frequency dependent channel fading is the result of reflections and multipath propagation. One main source for reflection and multipath propagation is impedance discontinuity. At impedance discontinuities part of the transmitted signal is reflected. The received signal is an addition of the reflected signal and original signal. The signal can be constructive or destructive, in which case signal fading may be generated. There are many possible reasons for impedance discontinuity, such as change of gauge of wires connected to each other, connected loads or branch wires, etc.

4.2. Influence of Load Impedance

This study is emphasized here because, it is common that the loads at the termination of branched lines are not always line characteristic impedance or resistive, rather it could be a case dependant arbitrary load, like, low or high impedance (R type) compared to line characteristic impedance and practical load impedance (RL type) representing transformers, machines, etc.

Domestic appliances connected to the power line network have impedances that are going to be decisive on the transfer function: the signal will either be absorbed by these impedances, or reflected on the network. These impedances vary with frequency and their impact of the transfer function will be significantly different.

Now, we consider the topology shown in figure 4 for studying the effect of load on the transfer function, which can be altered when connecting new load. The load impedances at point D in figure 1 were varied as 20 Ω, 50 Ω, 100 Ω, 200 Ω and characteristic impedance. The length of the branch BD is 10m.

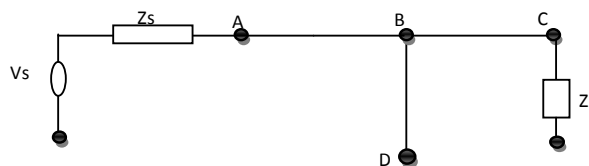


FIGURE 4: Power line network between sending and receiving ends

Figure 5 gives the transfer functions magnitudes measured by network analyzer in downlink from a household for the configurations below and between 1 MHz and 100 MHz. In the

presence of load impedances on the network, the channel attenuation is faster, especially in the case of 50 Ω where it reaches a value of -16 dB at 1 MHz.

For the load impedances less than channel characteristic impedance the position of notches is unchanged with no attenuation. It is interesting to observe that when the load impedance lowers the notches are at 40dB. As the load increase the peaks are increase and the notches decrease.

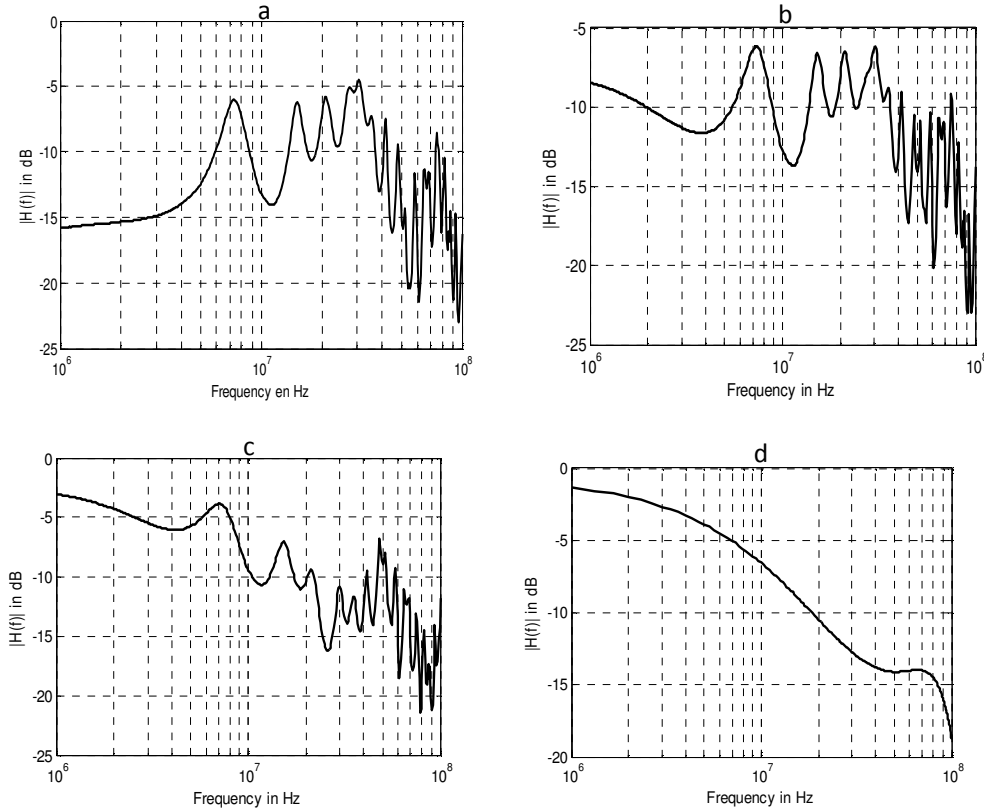


FIGURE 5: Experimental measurements of frequency response magnitude, (a) 50 Ω, (b) 100 Ω, (c) 200 Ω and (d) characteristic impedance

4.3. Simulation Results

The BER performance of CE-OFDM-CPM over PLC channel is evaluated using computer simulation. The parameters of the representative CE-OFDM-CPM system used for this study are demonstrated in Table I. The simulation results are performed with L = 15 length Hamming window FIR, having a normalized cutoff frequency $f_c = 0.4$.

M	Modulation order	4
$2\pi h$	Modulation index	0.3, 0.6, 0.8
N	Number of subcarriers	512
A	signal amplitude	1
J	Oversampling factor	4
N_B	Samples per symbol	2048
N_g	Samples per guard interval	384
N_F	Samples per frame	2432

TABLE 1: CE-OFDM-CPM parameters system

4.3.1. Effect of Impedance Loads on BER Simulation

The signal-to-noise ratio (SNR) is defined as E_b/N_0 , where E_b is the received energy per information bit and N_0 is the mono-lateral power spectral density.

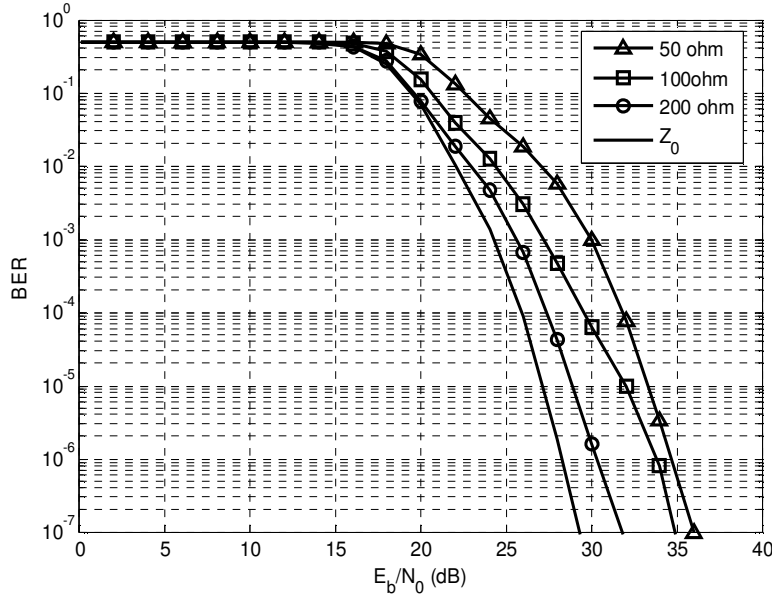


FIGURE 6: Simulation results for the CE-OFDM-CPM system with 4-QAM modulation for PLC channel for various load branch impedances ($2\pi h = 0.6$, $M=64$)

Figure 6, shows the performance of the CE-OFDM-CPM system for various load impedance cases. It is observed that the good performance can be obtained when the channel is terminated in characteristic impedances wherein the bit error probability is 10^{-7} at a E_b/N_0 per bit of 29 dB. The power is 32dB, 35dB and 36dB for 200 Ω , 100 Ω , and 50 Ω respectively. However, as the load impedance approaches a short circuit a degraded system performance is found. This is due to the fact that at short circuit, higher deep notches exist in the system. It is shown that the performance of PLC channel can be affected due to multipath phenomena. We have shown that the variations in the load terminations of those branches result in poor channel performances. On the other hand for lower terminal impedances in the range of few Ohm the channel shows a degraded performance. The findings presented in the paper can be used to improve the channel performance at design phase using interleaved coding techniques, channel precoding and channel equalizations methods, etc.

4.3.2. Effect of Modulation Order and Modulation Index on BER Simulation

Figure 7, shows simulation results for $M = 4, 8, 16, 32, 64$ and 128 . The bit error rate is plotted against the E_b/N_0 . There are two main observations to be made. The first, for a fixed modulation index, CE-OFDM-CPM has improved spectral efficiency with increase modulation order M at the cost of performance degradation. For example consider $2\pi h = 0.3$, the spectral efficiency is 2, 3, 4, 5, 6 and 7 b/s/Hz for $M = 4, 8, 16, 32, 64$ and 128 respectively. The second, from figure 7, it can be seen that with M increasing the system requires augmenting the E_b/N_0 in order to achieve a certain BER. For example consider $2\pi h=0.8$, if $M=4$, to achieve BER of 3.10^{-7} the E_b/N_0 need to be only about 23dB. And if $M=8, 16, 32, 64$ and 128 to achieve the same BER, the E_b/N_0 need to be 26 dB, 33 dB, 37 dB, 42 dB and superior to 50 dB respectively. So M should not take too large value when E_b/N_0 is limited. However, the larger M is, the higher the maximum data transmission rate of the system is.

In the case of $2\pi h=0.8$ it can be seen that, if let $BER \leq 10^{-6}$, the system can achieve about 32Mbit/s and 112Mbit/s data transmission rates when the SNR are about 22 dB and 48 dB respectively.

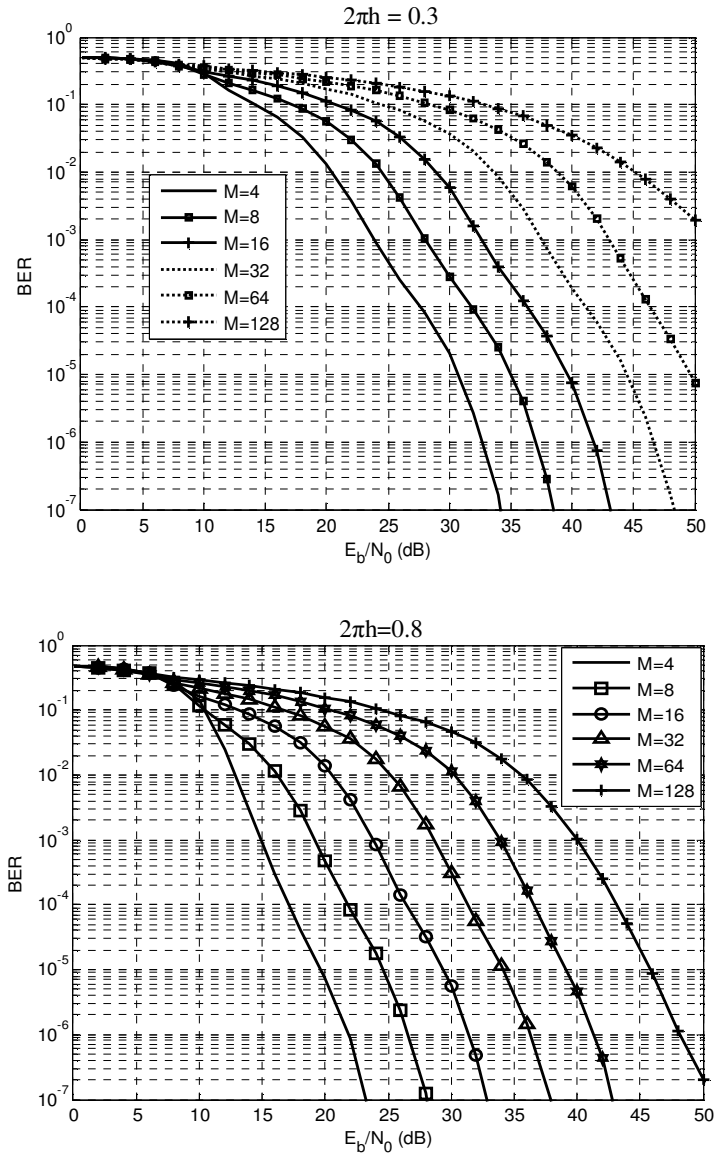


FIGURE 7: BER of CE-OFDM-CPM systems in PLC channel. (N=512, J=4, MMSE)

4.3.3. OFDM versus CE-OFDM

➤ Solid-State Power Amplifier Model

The nonlinear AM/AM characteristic of the solid-state power amplifier (SSPA) used in our simulations has been modeled by a memory less block with input-output relationship given by [17],

$$s'(t) = g[s(t)] = \frac{g_c |s(t)|}{\left(1 + \left(\frac{|s(t)|}{s_{sat}}\right)^{2p}\right)^{\frac{1}{2p}}} e^{j \arg\{s(t)\}} \quad (7)$$

Where g_c is the amplifier gain associated to a given peak-power P_p , the parameter p controls the smoothness of the transition from the linear region to the saturation region and s_{sat} is the saturation amplitude parameter, i.e., s_{sat} indicates at which amplitude the transition between linear and saturation region is located. The amplifier IBO is defined as

$$IBO = s_{sat}^2 / \sigma_s^2 \quad (8)$$

so that the reference power is determined by the saturation parameter s_{sat} . Following this IBO definition, IBO=0 dB represents a condition in which the power of signal at the input of the SSPA is $\sigma_s^2 = s_{sat}^2$, i.e., the input signal is characterized by dynamic greater than s_{sat} , driving heavily the SSPA into the saturation region. For CE-OFDM, the PAPR is 0 dB, and nonlinear distortion is avoided. CE-OFDM-CPM operates at IBO=0 dB, maximizing the range and efficiency of the PA [18]. For OFDM, $s(t)$ is Rayleigh distributed [19] resulting in a large PAPR. To avoid nonlinear distortion, large back-off is required, reducing range and PA efficiency [20], [21].

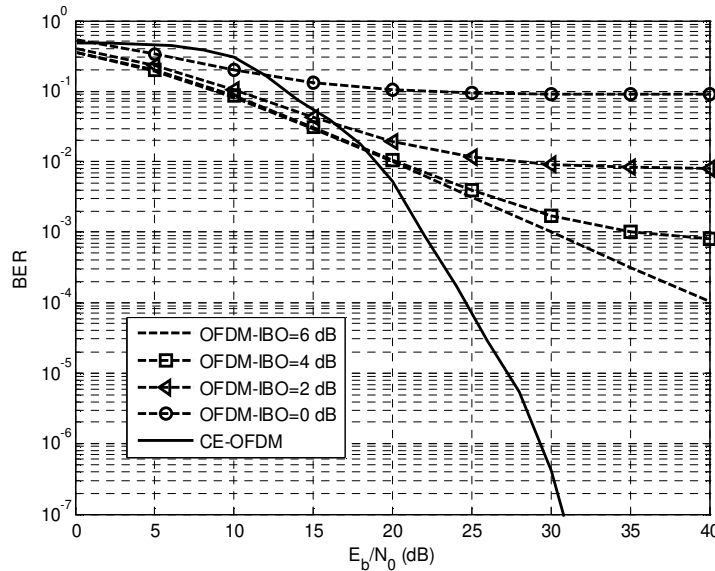


FIGURE 8: CE-OFDM-CPM versus OFDM under HomePlug 1.0

in power amplifiers (PA), the most efficient operating point is at the PA's saturation point, but for signals with large PAPR the operating point must shift to the left keeping the amplification linear. The average input power is reduced and consequently this technique is called input power back-off (IBO). At large back-off the efficiency of a power amplifier is very low. Such efficiency is detrimental to mobile battery-powered devices which have limited power resources. Here we assume that we need IBO 0=dB. In our simulation we considered AM/AM characteristic to model SSPA with peak-power $P_p=10$ W, $g_c=5$, $\rho=3$ and $S_{sat}=1.18$ w.

In figure 8, the performance of CE-OFDM-CPM is compared with the conventional OFDM over PLC channels under HomePlug 1.0, considering different values of IBO. In this case $2\pi h=0.8$ and $M=16$. Over the region $0\text{dB} \leq E_b/N_0 \leq 15\text{dB}$ and for $(IBO > 0\text{dB})$, the OFDM system performs better than the CE-OFDM-CPM system. However At high E_b/N_0 , CE-OFDM-CPM is shown to outperform OFDM. On the other hand, one can conclude that for IBO value of 0 dB the CE-OFDM-CPM system outperform the OFDM system: this is justified by the fact that the SSPA operates at a nonlinear point such that the OFDM signal is heavily distorted. As a consequence, the BER curves obtained with the OFDM system are affected by (i) errors generated by thermal noise, (ii) signal distortion.

Making a direct comparison between CE-OFDM-CPM and conventional OFDM is difficult due to the various parameters involved (M , $2\pi h$, IBO, etc.), and due to the fact that system requirements vary from system to system. For example, if power amplifier efficiency is the most important requirement, then the input power back-off of 0dB should be chosen. At this back-off level, the OFDM system has a very high irreducible error floor due to the power amplifier distortion, while the CE-OFDM-CPM system is relatively unaffected. Alternatively, if

operation at low E_b/N_0 is important, then CE-OFDM-CPM may not be well suited due to the threshold effect.

5. CONCLUSION

In this paper a transformation technique that eliminates the PAPR problem associated OFDM is developed. The phase modulation transform results in 0 dB PAPR constant envelope signals ideally suited for nonlinear, efficient amplification. The main advantage of the CE-OFDM-CPM is to reduce the PAPR to 0 dB which improves power efficiency and improvement in BER performance is achieved over conventional technique.

Results of BER simulations for different channel response are presented. As the terminal impedances on the branches increase to line characteristic impedance, the signal attenuation and distortions tend to reduce. CE-OFDM is shown to compare favorably to conventional OFDM in PLC channels when the impact of nonlinear power amplification is taken into account. CE-OFDM-CPM is also shown to suffer from the FM threshold effect, however. Potential solutions to this problem, including threshold extension with phase locked loops, are discussed.

6. REFERENCES

- [1] V. Degardin, M. Lienard, A. Zeddou, F. Gauthier, and P. Degauque, "Classification and Characterization of Impulsive Noise on Indoor Power Line used for Data Communication," IEEE Transactions on Consumer Electronics, vol. 48, no. 4, pp. 913–918, November 2002.
- [2] F. J. Canete, L. Diez, J. A. Cortés, and J. T. Entrambasaguas, "Broad-Band Modeling of Indoor Power Line channels," IEEE Transactions on Consumer Electronics, pp. 175–183, Feb 2002.
- [3] M. Tlich, A. Zeddou, F. Moulin, and F. Gauthier, "Indoor Power Line communications Channel Characteristic Model," IEEE Transaction on power delivery, vol.23,no.3,pp.1392–1401,July2008.
- [4] M. Zimmermann and K.Dostert, "Analysis and Modeling of Impulsive Noise in Broad-Band Power Line communications," IEEE Transactions on Electromagnetic Compatibility, vol. 44, no. 1, pp. 249–258, February 2002.
- [5] R. Prasad, "OFDM for Wireless Communications System ", Boston, MA, Artech House, 2004.
- [6] Ma Y H, So P L, Gunawan E. "Performance Analysis of OFDM system for Broad-Band Power Line Communications Under Impulsive Noise and Multipath Effects". IEEE Transactions on Power Delivery, 2005, 20(2): 674-682.
- [7] P. Amirshashi, S. M. Navidpour and M. Kavehrad, "Performance Analysis of Uncoded and Coded OFDM Broad-Band Transmission Over Low Voltage Power Line Channels with Impulsive Noise ", IEEE Transactions on Power Delivery, Vol. 21, No. 4, October, 2006.
- [8] J. Sun Lee; H. Oh; J. Kim; J. Y. Kim; "Performance of Scaled SLM for PAPR Reduction of OFDM signal In PLC channels" Power Line Communications and Its Applications, 2009, ISPLC 2009, IEEE International Symposium.
- [9] S. Yoo, S. Yoon, S. Yong Kim, I. Song, "A Novel PAPR Reduction Scheme for OFDM Systems: Selective Mapping of Partial Tones (SMOPT)", IEEE Transactions on Volume 52, Issue 1, Date: Feb. 2006, Pages: 40 - 43.
- [10] P. O. Börjesson, H. G. Feichtinger, N. Gijc, M. Isaksson, N. Kaiblinger, P. Lindling, L. Persson, "A Low Complexity PAPR Reduction Method for DMT-VDSL", 5th International Symposium on Digital Signal Processing for Communication Systems (DSPCS'99), pages 164–169, Perth, Australia, Feb. 1999.

- [11] S.C. Thompson, "Constant Envelope OFDM Phase Modulation," Ph. D. dissertation, University of California, San Diego, 2005. [Online]. Available: <http://zeidler.ucsd.edu/~sct/thesis/>.
- [12] Steve C. Thompson, Ahsen U. A, John G. Proakis, James R. Zeidler and Michael J. Geile, "Constant Envelope OFDM", IEEE Trans. On communication. VOL. 56, NO. 8, AUGUST 2008.
- [13] M. El Ghzaoui, J. Belkaidid, A. Benbassou, "Performance Evaluation of CE-OFDM in PLC Channel" SPIJ February 2011 Volume: 4 Issue: 6.
- [14] S. C. Thompson, J. G. Proakis, and J. R. Zeidler. "Non-coherent Reception of Constant Envelope OFDM In Flat Fading". In Proceedings of the IEEE 16th International Symposium on PIMRC, Baltimore, MD, USA, 2005.
- [15] K. Dostert, "Power Line Communications", Prentice-Hall, 2001.
- [16] Y. Tsai and G. Zhang, "Orthogonal Frequency Division Multiplexing with Phase Modulation and Constant Envelope Design," in Proc. of IEEE Milcom 2005, Atlantic City, NJ, Oct. 2005.
- [17] C. Rapp, "Effects of HPA-Nonlinearity On A 4-DPSK/OFDM signal for A Digital Sound Broadcasting System," in Proc. European Conf. Satellite Commun. (ECSC'91), Vol. 1, October 1991, pp. 179–184.
- [18] F. H. Raab, P. Asbeck, S. Cripps, P. B. Kenington, Z. B. Popovic, N. Potheary, J. F. Sevic, and N. O. Sokal, "Power Amplifiers and Transmitters for RF and Microwave," IEEE Trans. Microwave Theory Tech., vol. 50, no. 3, pp. 814–826, Mar. 2002.
- [19] S. Shepherd, J. Orriss, and S. Barton, "Asymptotic Limits in Peak Envelope Power Reduction by Redundant Coding in Orthogonal Frequency Division Multiplex Modulation," IEEE Trans. Commun., vol. 46, no. 1, pp.5–10, Jan.1998.
- [20] C. P. Liang, J. H. Jong, W. E. Shark, and J. R. East, "Nonlinear Amplifier Effects in Communications Systems," IEEE Trans. Microwave Theory Tech., vol. 47, no. 8, pp. 1461–1466, Aug. 1999.

An Approach to Reduce Noise in Speech Signals Using an Intelligent System: BELBIC

Edet Bijoy K

*Department of ECE
MES College of Engineering
Kuttippuram, 679573, Kerala, India*

edetbijoyk@ieee.org

Musfir Mohammed

*Department of ECE
MES College of Engineering
Kuttippuram, 679573, Kerala, India*

mohammed.musfir@ieee.org

Abstract

The two widespread concepts of noise reduction algorithms could be observed are spectral noise subtraction and adaptive filtering. They have the disadvantage that there is no parameter to distinguish between the speech and the noise components of same frequency. In this paper, an intelligent controller, BELBIC, based on mammalian limbic Emotional Learning algorithms is used for increasing the speech quality from a noisy environment. Here the learning ability to train the system to recognize and the output thus obtained would be the fundamental frequency of the speech spectrum thus reducing the noise level to minimum. The parameters on which the reduction of noise from the input speech spectrum depends have also been studied. The real time implementations have been done using Simulink and the results of the analysis thus obtained are included in the end.

Keywords: BELBIC, Spectral Noise, Adaptive Filtering, Fundamental Frequency, Simulink

1. INTRODUCTION

In recent years, two widespread concepts of noise reduction algorithms could be observed: spectral noise subtraction and adaptive filtering. The former has the drawback of generating residual noise with musical character, the so-called musical noise, while the latter distorts the frequency and phase response of speech signals [1,2]. In addition, both methods fail to enhance speech recordings disturbed by loud hum (50 Hz or 60 Hz) because their analysis windows enlarge the line spectrum by significant artificial side lobes. Here an attempt is made to cancel the noise from the surrounding environment to improve the quality of the speech and the avail of speech analysis in its fundamental frequency using a self learning Brain Emotion Learning system which works by mimicking the action of the mammalian limbic system.

Emotional Learning is a psychologically motivated algorithm which is a family of intelligent algorithms. Recently, biologically motivated intelligent computing has been successfully employed for solving different types of problems. The greatest different of an intelligent system from a traditional one is the capability of learning. A common attribute of the learning process is the adaptation of the system parameters to better tackle the changing environment. An evaluation mechanism is necessary that any learning algorithm assesses the operating condition of the system. One type of evaluation is based on emotional cues, which evaluate the impact of the external stimuli on the ability of the system both to function effectively in the short term and to maintain its long term prospects for survival [3]. Emotional learning is one of the learning strategies based on emotional evaluations. In mammalian brains, this learning process occurs in the brain Limbic System. The paper includes a short overview of the biological concepts followed by a detailed study of the architecture including the algorithm of the model. The results obtained from the real time implementation in Simulink are discussed towards the end.

2. BELBIC

Moren and Balkenius [4,5] presented a neurologically inspired computational model of the Amygdala and the Orbitofrontal Cortex in the Limbic System. Based on this model, a control algorithm called Brain Emotional Learning Based Intelligent Controller (BELBIC) has been suggested [6]. The two approaches of applying the brain emotional learning model into control systems are direct approach and indirect approach. The former uses BEL model as the controller block, while the latter utilizes BEL model to tune the controller parameters. In this work the BEL model itself is used as the controller. In real time control and decision systems, Emotional Learning is a powerful methodology due to its simplicity, low computational complexity and fast training where the gradient based methods and evolutionary algorithms are hard to be applied because of their high computational complexity [7]. The BELBIC has been designed for SISO applications and for MIMO systems, one must employ each controller for generating one control output. The relevant researches have indicated that BELBIC has a good robustness and performance.

2.1 Architecture of the Limbic System

The Limbic System, as part of the mammalian creatures' brain, is mainly in charge of the emotional processes. The Limbic System located in the cerebral cortex consists mainly of following components: Amygdala, Orbitofrontal Cortex, Thalamus, Sensory Cortex, Hypothalamus, Hippocampus and others of which the Amygdala and Orbitofrontal Cortex are of importance in our model. Fig. 1 illustrates the anatomy of the main components of Limbic System [8].

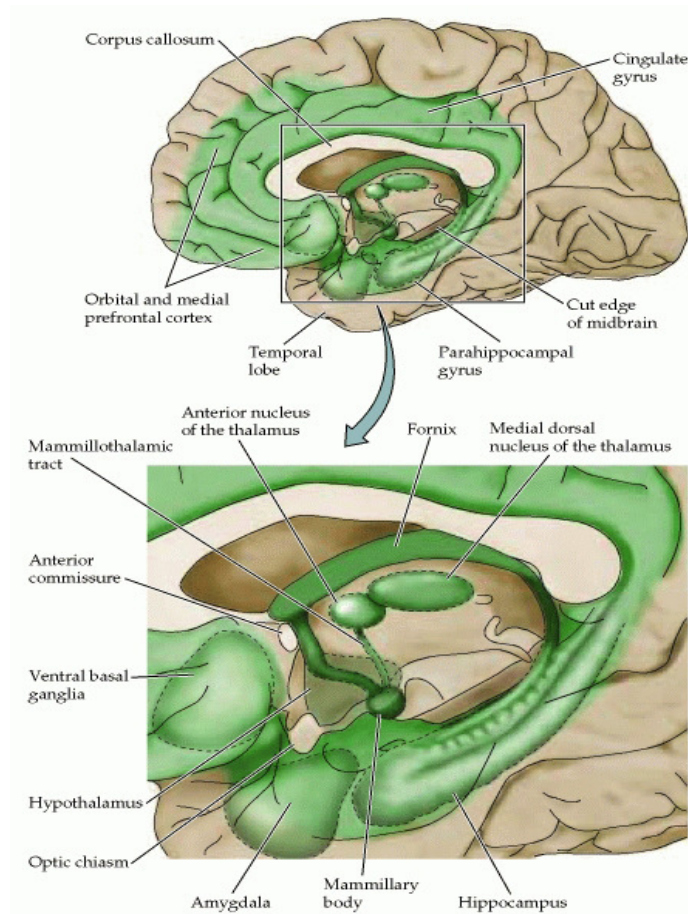


FIGURE 1: The major brain structures associated with the Limbic System

In this section these main components are discussed in detail. The first sign of affective conditioning of the system appears in Amygdala which is a small almond-shaped in sub-cortical area. This component is placed in a way to communicate with all other Sensory Cortices and areas within the Limbic System. The Amygdala connections to/from other components are illustrated in Fig. 2 [5]. The studies show that a stimulus and its emotional consequences are associated in the Amygdala area [9]. In this region, highly analyzed stimuli in the Sensory Cortices, as well as coarsely categorized stimuli in the Thalamus are associated with an emotional value.

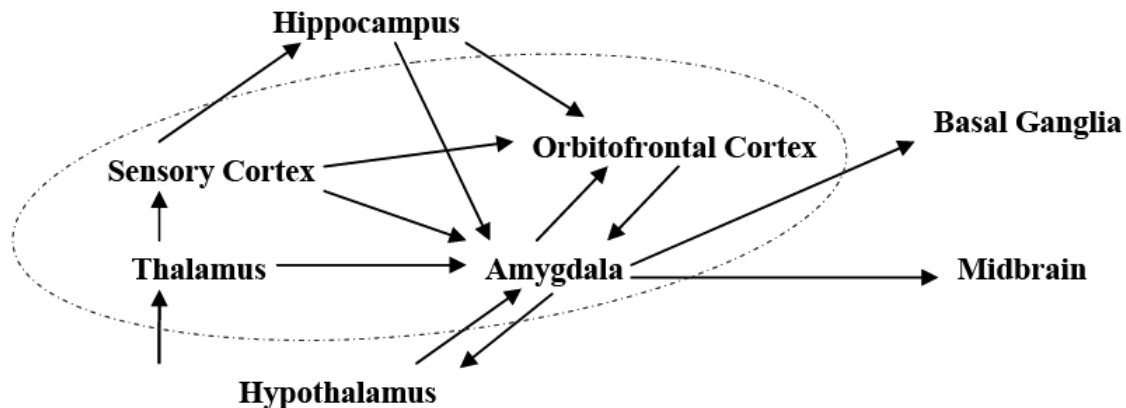


FIGURE 2: Connections of the Amygdala with other components of the Limbic System.

The Orbitofrontal Cortex, as of another component of the brain system, interacts with the Amygdala. The main interrelated function of this component is: Working Memory, Preparatory Set and Inhibitory Control [9]. The current and recent past events are represented in the Working Memory. The Preparatory Set is the priming of other structures in anticipation of impending action. Inhibitory Control is the selective suppression of areas that may be inappropriate in the current situation. More specifically, the Orbitofrontal Cortex takes action in omission of the expected reward or punishment and control the extinction of the learning in the Amygdala [9].

Another component in this area is Thalamus which lies next to the basal ganglia. It is a non-homogeneous sub-cortical structure and a way-station between cortical structures and sub-cortical. Moreover, various parts of the Thalamus also relay the majority of sensory information from the peripheral sensory systems to the Sensory Cortices. The Thalamus signal going to the Amygdala evades the processes involved in the Sensory Cortex and other components of the system. Therefore, Amygdala receives a non-optimal but fast stimulus from the Thalamus which among the input stimuli is often known as a characteristic signal.

The next component is the Sensory Cortex close to the Thalamus which receives its input from the latter one. In fact, Sensory Cortex processes the information from the sensory areas. The Sensory Cortex sends highly analyzed input to the Amygdala and Orbitofrontal [9]. Generally, the mammals use these areas of their Limbic System for higher perceptual processing.

2.2 Computational Model of the BEL

Moren and Balkenius [4,5] developed a computational model that mimics Amygdala, Orbitofrontal Cortex, Thalamus, Sensory Input Cortex and generally those parts of the brain thought responsible for processing emotions. Fig. 3 shows the computational model of emotional learning [4]. The model is divided into two parts: the Amygdala and the Orbitofrontal cortex. The Amygdala part receives inputs from the Thalamus and from cortical areas, while the Orbitofrontal obtains

inputs from the cortical areas and the Amygdala. The system also receives a reinforcing signal (Primary Reward).

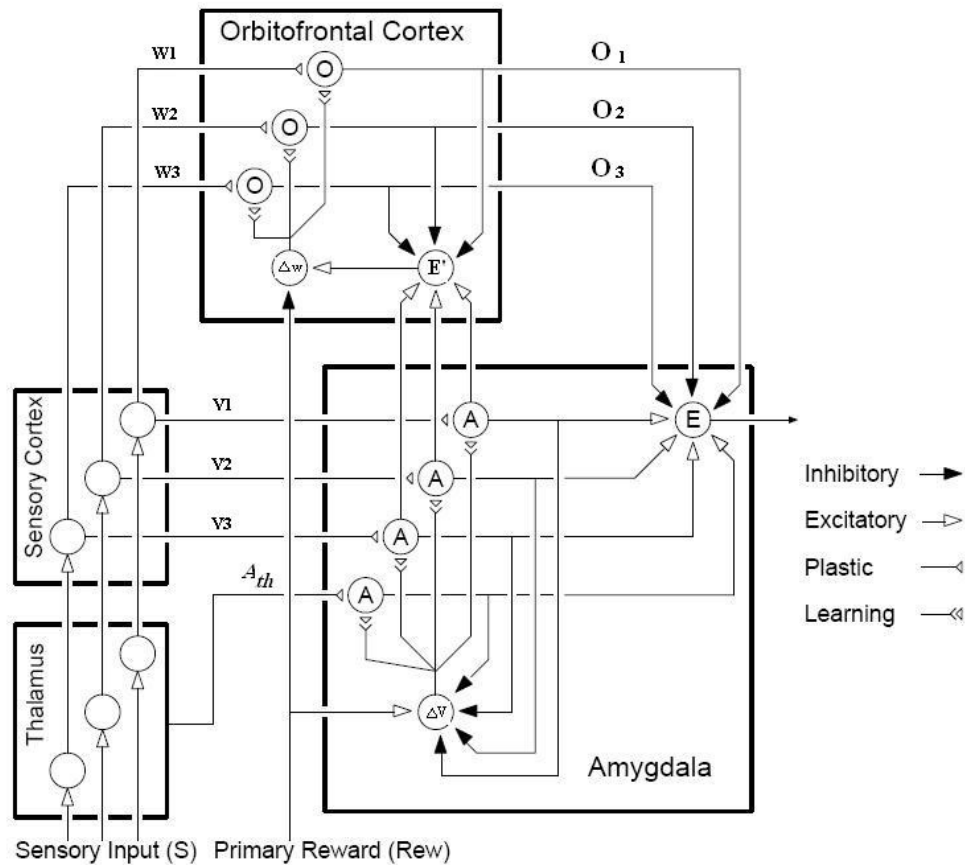


FIGURE 3: Graphical depiction of the Brain Emotional Learning (BEL) process

The vector S shows stimuli inputs to the system. There is one A node for each stimulus S . A_{th} is another input to the Amygdala part which is the maximum of stimuli inputs(S):

$$A_{th} = \max (S_i) \quad (1)$$

There is a plastic connection weight V for each A node. The output of each node obtains by multiplying any input with the weight V .

$$A_i = S_i V_i \quad (2)$$

The V_i is adjusted proportionally to the difference between the activation of the A nodes and the reinforcement signal Rew . The α term is a constant used to adjust the learning speed:

$$\Delta V_i = \alpha (S_i \max(0, Rew - \sum_j A_j)) \quad (3)$$

The weights V cannot decrease. It is good reasons for this design choice because once an emotional reaction is learned, this should be permanent and cannot be unlearned. It is the task of the Orbitofrontal part to inhibit this reaction when it is inappropriate. The Orbitofrontal learning rule is very similar to the Amygdala rule but the Orbitofrontal connection weight can both increase and decrease. The O nodes behave analogously, with a connection weight W employed to the input signal to create an output.

$$O_i = S_i W_i \tag{4}$$

β is another learning rate constant. ΔW_i is calculated as:

$$\Delta W_i = \beta (S_i (E' - Rew)) \tag{5}$$

The E node sums the outputs from the A nodes and then subtracts the inhibitory outputs from the O nodes. The result is the output from the model. The A nodes give outputs proportionally to their contribution in predicting the reward Rew , while the O nodes inhibit the output of E as necessary. The E' node is sums of the outputs from A except A_{tr} and then subtract from inhibitory outputs from the O nodes.

$$E = \sum_i A_i - \sum_i O_i \text{ (including } A_{tr}) \tag{6}$$

$$E' = \sum_i A_i - \sum_i O_i \text{ (not including } A_{tr}) \tag{7}$$

Based on the above equations the BELBIC model was designed as a cognitively open loop model by C. Lucas et al [6]. Fig 4 is the implementation of the foresaid model [6]. The BELBIC is essentially an action generation mechanism based on sensory inputs and emotional cues (Reward signals). The BELBIC equations are the mentioned formulas of (1) - (7). The main issue in using the model for different applications is defining the sensory and emotional signals in such a way that properly represent the state and objectives of the system.

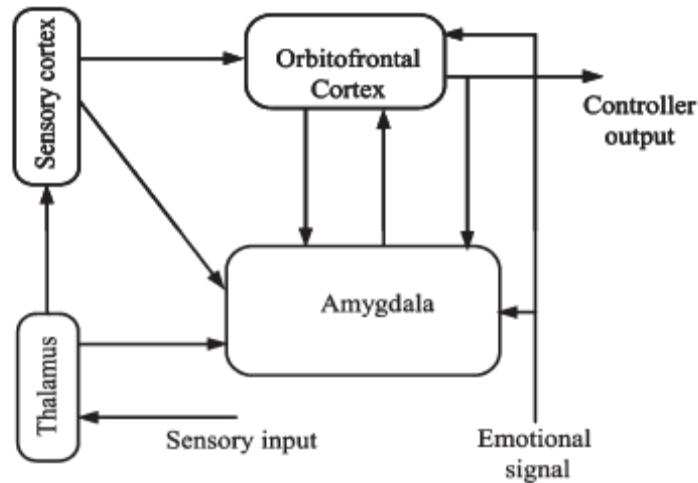


FIGURE 4: Basic block structure of emotional controller

Fig. 5 demonstrates a reasonable candidate for embedding the BELBIC model within a typical feedback control block diagram [6]. The implemented functions in emotional cue and sensory input blocks should be defined for each application.

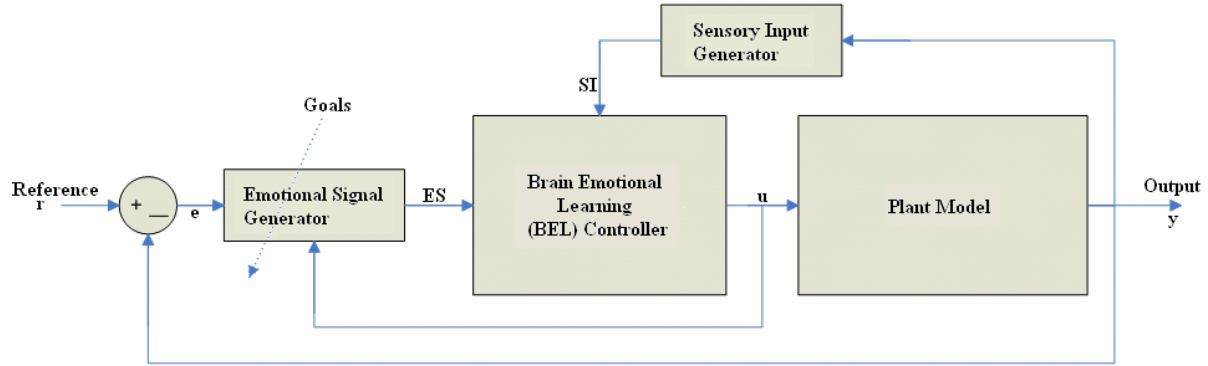


FIGURE 5: Control system configuration using BELBIC

3. APPLICATION OF BELBIC FOR NOISE REDUCTION

The above model is implemented in the obtaining of the speech signals from a noisy environment. The real time implementation is done using Matlab2006b. Fig 6 shows the block structure implemented in Simulink.

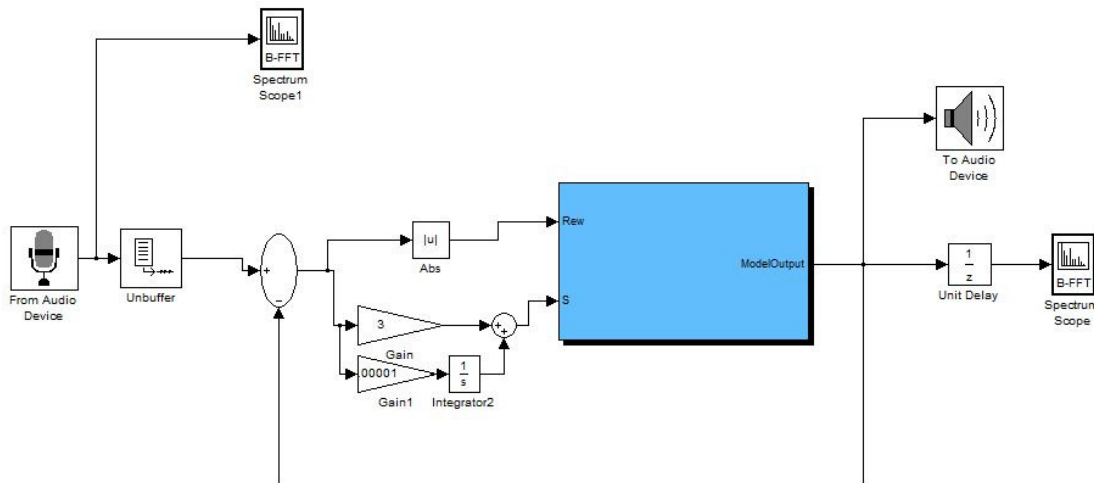


FIGURE 6: Implementation of noise elimination system in Simulink

Male voice sampled at a frequency of 1000Hz is given as the speech input through the microphone from a room environment. Noisy environment is ensured with other sound sources at varying frequencies. The Reward signal consisted of the absolute value of the speech input. The sensory input is taken as the sum of the speech input and its integral. The negative feedback is provided for the stability of the system. The system tries to attain more of the reward from the input by giving the output of the most prominent fundamental frequencies of the speech signal and suppressing the other. Thus the hum produced due to the harmonics is very negligible. The gain control is achieved due to the negative feedback present in the system and the integral component to the sensory input.

3.1 Results

The simulation results are as shown for varied gain parameters of the speech and the integral input respectively.

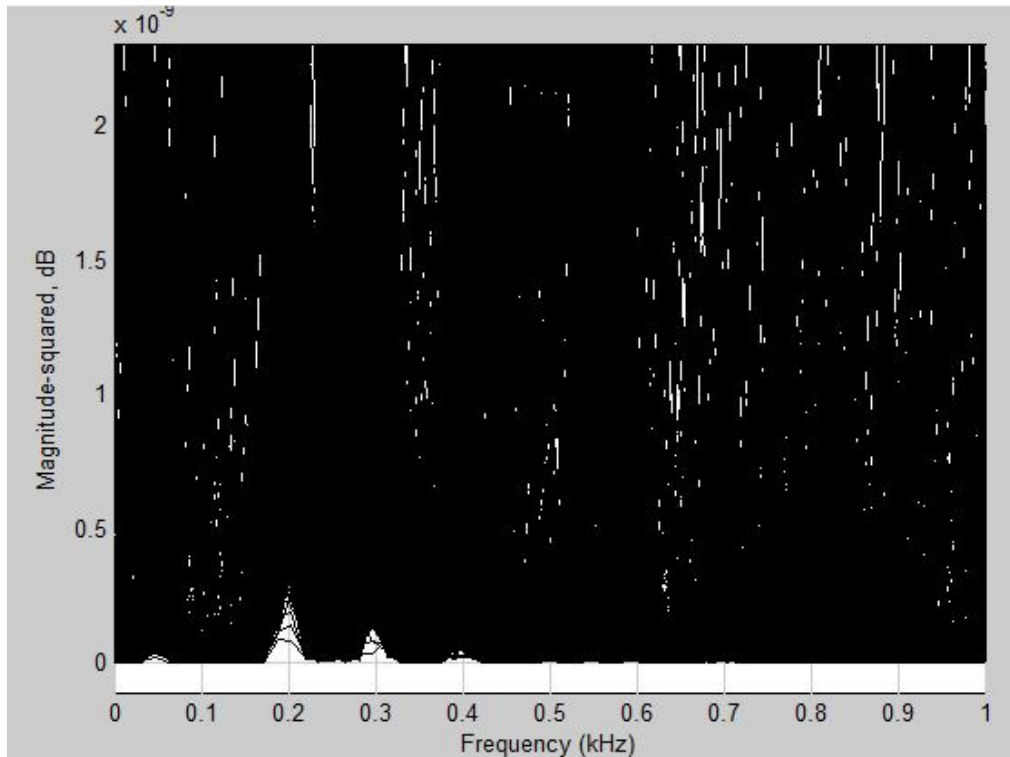


FIGURE 7: Spectrum of the speech input to the system

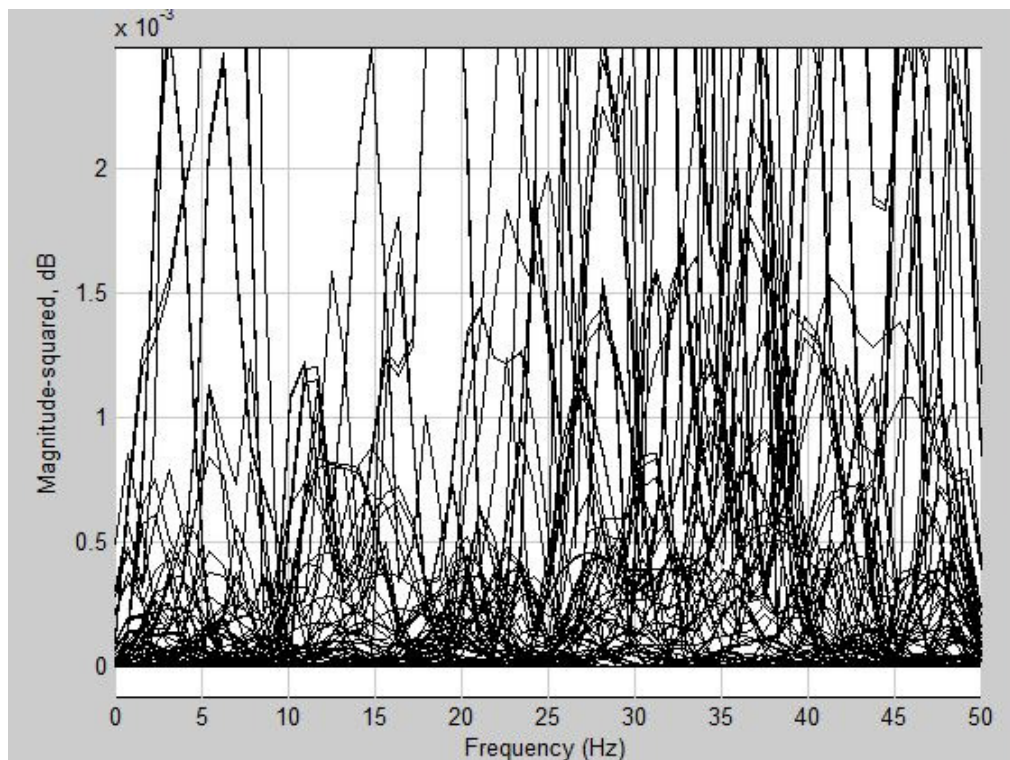


FIGURE 8: Output for gains 1 and 0

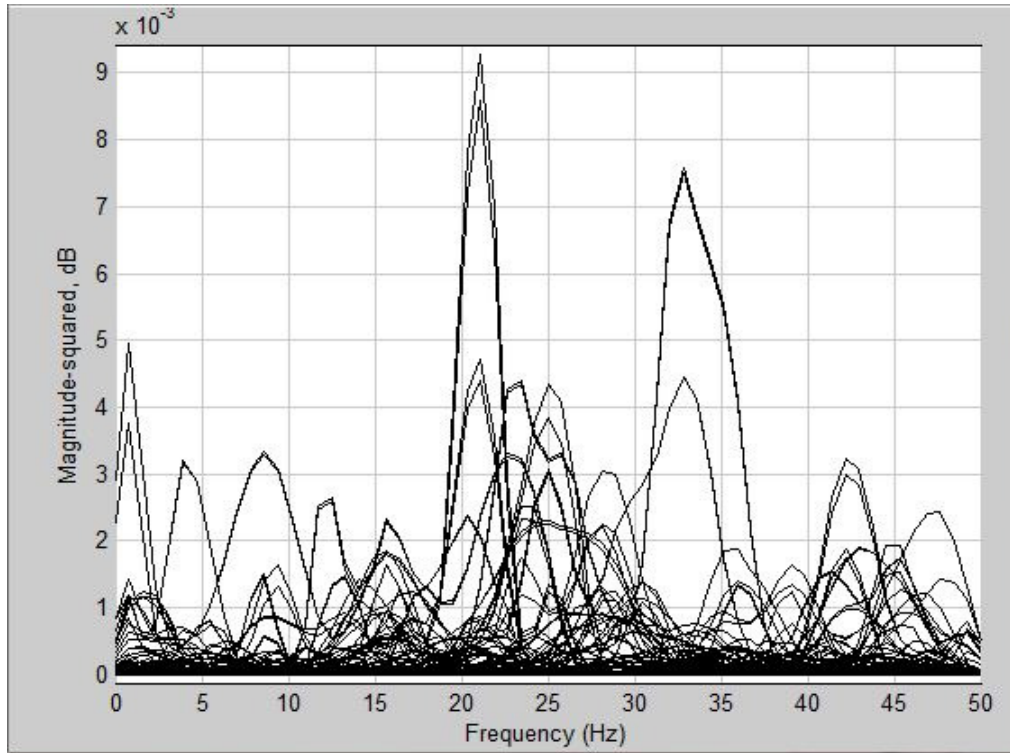


FIGURE 9: Output for gains 1 and 0.00001

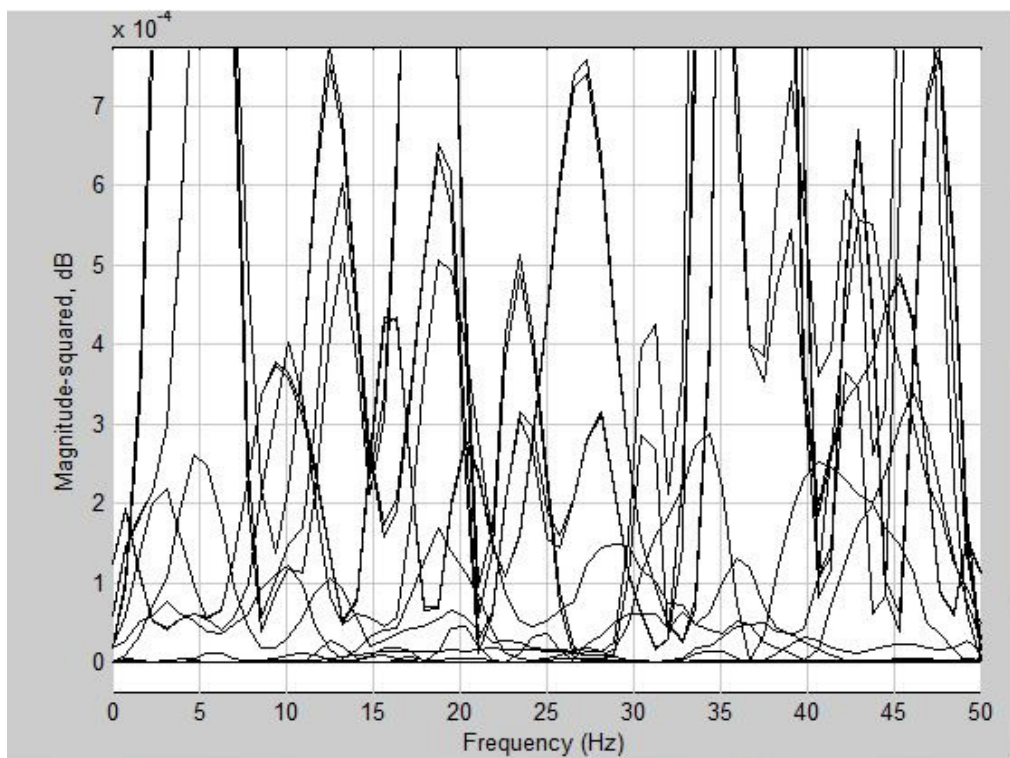


FIGURE 10: Output for gains 1 and 10

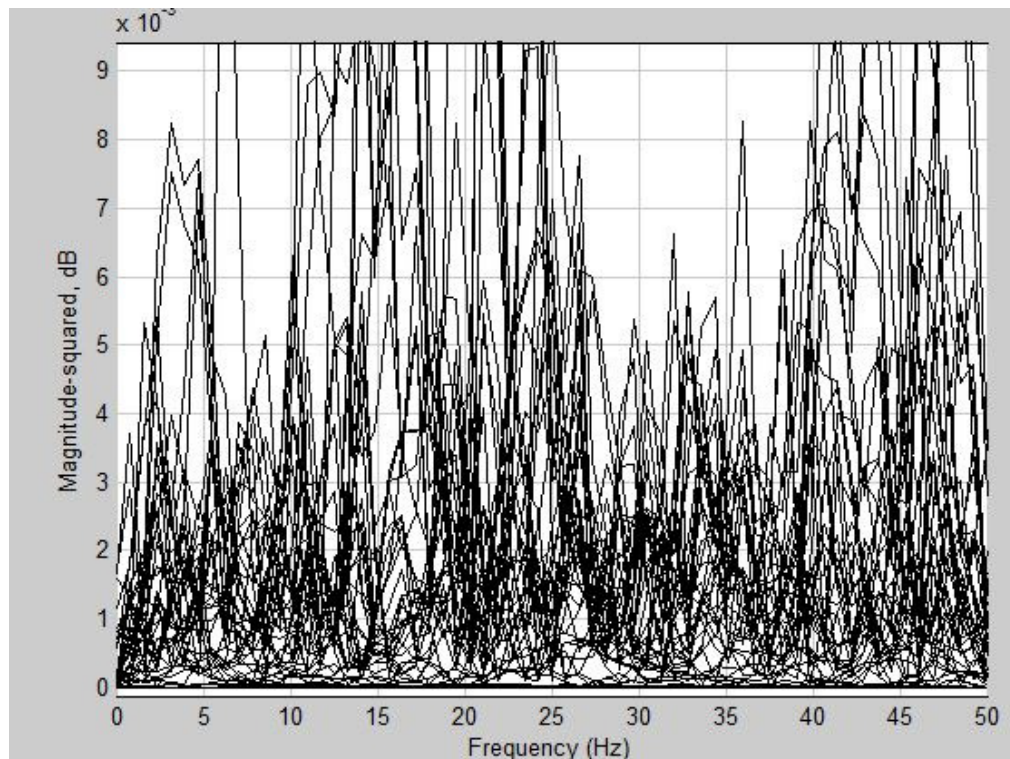


FIGURE 11: Output for gains 100 and 2

Fig. 7 shows the spectrum of the input speech in which the noise and the harmonics are very prominent. Fig. 8 is the output without the integral component to the sensory input. The output quality is further increased when the integral component gain is .00001 as in fig 9. Fig. 10 shows the output for a gain of 10 for the integral component. Fig 11 is when the speech component has a gain of 100 and the integral component 2. From the above results it can be seen that the quality of noise elimination increases with the increase in integral gain. This cannot be increased above a particular limit as the learning ability of the system reduces i.e. the learning period increases thus causing a delay in the transmission of the output. The easy learning property of the system is to be exploited in this system. The increase in the gain of the speech component increases the learning capability over an undesirable rate and thus causes the repetition of the speech thus affecting the quality.

The inputs given have a noisy component which is the original speech signal and the integrated signal which contains the lower frequency component. The gain of this lower frequency signal is the determining parameter as it is the signal with lesser noise and more of speech component. Further the integrated signal also functions in tuning the learning ability of this system at a desirable speed. A higher gain for the low frequency signal ensures a higher quality in the speech output but is limited by the learning capability of the system.

Noise reduction using this system requires only preliminary knowledge of the elements of speech spectrum. There have been approaches made using analogous controllers where a Voice Activity Detection (VAD) is necessary to prevent noise amplification. VAD being computationally intensive requires a very complex algorithm [10]. Using a system of high learning ability such as BELBIC saves this complexity. Furthermore as the learning method is emotional learning the algorithm is very simple. The efficiency of the BELBIC controller over the analogous counterparts such as the PID controller is very high due to the high intelligence. Thus the responses of this controller are faster and with less overshoots compared with those of the PID counterparts [3].

4. CONCLUSION

BELBIC is a highly versatile intelligent system. It has a very high degree of accuracy and disturbance handling ability due to appropriate learning ability compared to analogous classical controllers. In this work as the fundamental frequency of speech is prominent in the output this can be implemented in the voice recognition systems and other high end speech applications. The algorithm being based on emotion learning is very versatile and easy to implement. The work is to be extended for implementation in DSK TMS320C6713. Applications of this type of systems can be in hearing aids, speech synthesis systems communication systems in noisy environment etc.

5. REFERENCES

- [1]. Yoma, N. B.; McInnes, F. R.; Jack, M. A. (1997). "Spectral subtraction and mean normalization in the context of weighted matching algorithms." *In Proc. of EUROSPEECH '97, vol. 3, pp. 1411–1414, Rhodes; Greece.*
- [2]. Pfitzinger, H. R. (1998). "The collection of spoken language resources in car environments." *In ICLRE '98, vol. 2, pp.1097–1100, Granada; Spain.*
- [3]. D. Shahmirzadi, "Computational Modeling Of The Brain Limbic System And Its Application In Control Engineering", *Master dissertation, Texas A&M University, U.S.A. , (2005).*
- [4]. J. Moren, C. Balkenius, "A Computational Model of Emotional Learning in the Amygdala", *Cybernetics and Systems, Vol. 32, No. 6, (2000), pp. 611- 636.*
- [5]. J. Moren, "Emotion and Learning – A Computational Model of the Amygdala", *PhD dissertation, Lund University, Lund, Sweden, (2002).*
- [6]. C. Lucas, D. Shahmirzadi, N. Sheikholeslami, "Introducing BELBIC: Brain Emotional Learning Based Intelligent Controller", *International Journal of Intelligent Automation and Soft Computing, Vol. 10, NO.1, (2004), pp. 11- 22.*
- [7]. R. Ventura, and C. Pinto Ferreira, "Emotion based control systems", *Proc. Of IEEE Int. symp. On Intelligent control/Intelligent systems and semiotics, Cambridge, MA, (1999), pp. 64-66.*
- [8]. D. Purves, G. J. Augustine, D. Fitzpatrick, L. C. Katz, A. LaMantia, J. O. McNamara, S. M. Williams, "Neuroscience" , *Sinauer Associates, (2001).*
- [9]. E. T. Rolls, "A Theory of Emotion and Consciousness, and Its Application to Understanding the Neural Basis of Emotion." *Cambridge, MA: MIT Press. (1995).*
- [10]. G.S. and Lidd, M.L., "Automatic gain control. Acoustics, Speech, and Signal Processing Kang", *IEEE International Conference on ICASSP. Volume 9,1984, pp. 120 – 123.*

INSTRUCTIONS TO CONTRIBUTORS

The *International Journal of Signal Processing (SPIJ)* lays emphasis on all aspects of the theory and practice of signal processing (analogue and digital) in new and emerging technologies. It features original research work, review articles, and accounts of practical developments. It is intended for a rapid dissemination of knowledge and experience to engineers and scientists working in the research, development, practical application or design and analysis of signal processing, algorithms and architecture performance analysis (including measurement, modeling, and simulation) of signal processing systems.

As SPIJ is directed as much at the practicing engineer as at the academic researcher, we encourage practicing electronic, electrical, mechanical, systems, sensor, instrumentation, chemical engineers, researchers in advanced control systems and signal processing, applied mathematicians, computer scientists among others, to express their views and ideas on the current trends, challenges, implementation problems and state of the art technologies.

To build its International reputation, we are disseminating the publication information through Google Books, Google Scholar, Directory of Open Access Journals (DOAJ), Open J Gate, ScientificCommons, Docstoc and many more. Our International Editors are working on establishing ISI listing and a good impact factor for SPIJ.

The initial efforts helped to shape the editorial policy and to sharpen the focus of the journal. Starting with volume 5, 2011, SPIJ appears in more focused issues. Besides normal publications, SPIJ intend to organized special issues on more focused topics. Each special issue will have a designated editor (editors) – either member of the editorial board or another recognized specialist in the respective field.

We are open to contributions, proposals for any topic as well as for editors and reviewers. We understand that it is through the effort of volunteers that CSC Journals continues to grow and flourish.

SPIJ LIST OF TOPICS

The realm of Signal Processing: An International Journal (SPIJ) extends, but not limited, to the following:

- Biomedical Signal Processing
- Communication Signal Processing
- Detection and Estimation
- Earth Resources Signal Processing
- Industrial Applications
- Optical Signal Processing
- Radar Signal Processing
- Signal Filtering
- Signal Processing Technology
- Software Developments
- Spectral Analysis
- Stochastic Processes
- Acoustic and Vibration Signal Processing
- Data Processing
- Digital Signal Processing
- Geophysical and Astrophysical Signal Processing
- Multi-dimensional Signal Processing
- Pattern Recognition
- Remote Sensing
- Signal Processing Systems
- Signal Theory
- Sonar Signal Processing
- Speech Processing

CALL FOR PAPERS

Volume: 6 - **Issue:** 1 - February 2012

i. Paper Submission: November 30, 2011

ii. Author Notification: January 01, 2012

iii. Issue Publication: January / February 2012

CONTACT INFORMATION

Computer Science Journals Sdn Bhd

B-5-8 Plaza Mont Kiara, Mont Kiara
50480, Kuala Lumpur, MALAYSIA

Phone: 006 03 6207 1607
006 03 2782 6991

Fax: 006 03 6207 1697

Email: cscpress@cscjournals.org

CSC PUBLISHERS © 2011
COMPUTER SCIENCE JOURNALS SDN BHD
M-3-19, PLAZA DAMAS
SRI HARTAMAS
50480, KUALA LUMPUR
MALAYSIA

PHONE: 006 03 6207 1607
006 03 2782 6991

FAX: 006 03 6207 1697
EMAIL: cscpress@cscjournals.org